VARIATIONAL STUDY OF SU(2) HAMILTONIAN LATTICE GAUGE THEORY USING BOTH ANALYTICAL AND BIASED-SELECTION MONTE CARLO INTEGRATION TECHNIQUES

By

MING C. HUANG

A DISSERTATION PRESENTED TO THE GRADUATE SCHOOL
OF THE UNIVERSITY OF FLORIDA IN
PARTIAL FULFILLMENT OF THE REQUIREMENTS
FOR THE DEGREE OF DOCTOR OF PHILOSOPHY

UNIVERSITY OF FLORIDA

1988

ACKNOWLEDGMENTS

First I would like to thank the chairman of my supervisory committee, Dr. F. E. Dunnam, for supporting me during the undertaking of this project. Without his support I would never have been able to continue in the field.

I also would like to thank the cochairman of my committee, Dr. R. L. Coldwell, who professed confidence in me and opened another research window for me. It has been joyful to sit with him and discuss physics. I have benefitted very much from his remarkable research experience.

Dr. M. W. Katoot provided my first introduction to the field. He worked very hard to create a research environment for me and has contributed helpful suggestions during the research.

Thanks go also to Drs. D. Robson and C. Long of Florida State University for their valuable guidance and many suggestions. As members of one of the most active research groups in the Hamiltonian lattice gauge theories, they shared with me many calculation results prior to publication without any reservation. I also greatly appreciate their encouragement.

As a non-American student, I would like to thank my teachers in the Department of Physics for the academic training they have provided me, of which I will always be very proud. I also would like to thank several faculty members in the Department for allowing me to participate in their research activities: Dr. H. Monkhorst, with whom I worked in the application of coupled-cluster method to the polymer system from 1982 to 1983, Dr. P.

Sikivie who shared his experience in axion physics and dark matter from 1983 to 1986, and Dr. J. McCabe, who worked with me in superstring theories from 1985 to 1986. Particularly, I would like to express my deep appreciation to Dr. Sikivie from whom I learned the importance of establishing my own research style.

The Space Astronomy Laboratory has been very kind to allow me to use its facilities to carry out this project.

I thank Mr. Frank Yacenda for spending a lot of time in editing my dissertation, Ms. Wendy Thornton for her assistance in preparing my dissertation in its final form and Ms. Stephanie Sanchez for her assistance in preparing the figures of my dissertation.

Finally, I wish to thank my wife Tsai-Yin and the members of my family for their understanding and support during a most difficult period of my life.

TABLE OF CONTENTS

Abstract of Dissertation Presented to the Graduate School
of the University of Florida in Partial Fulfillment of the
Requirements for the Degree of Doctor of Philosophy

VARIATIONAL STUDY OF SU(2) HAMILTONIAN LATTICE GAUGE THEORY USING BOTH ANALYTICAL AND BIASED-SELECTION MONTE CARLO INTEGRATION TECHNIQUES

By

Ming C. Huang

August 1988

Chairman: F. E. Dunnam
Major Department: Physics

SU(2) Hamiltonian lattice gauge theory is used as a theoretical model to test new computational methods developed in this dissertation and to study the possible features exhibited by Hamiltonian lattice QCD.

The basic method used here to study SU(2) Hamiltonian lattice gauge theory is a variational calculation, which enables non-perturbative calculations to be made from the strong-coupling region down to the scaling region. Expectation values of physical observables are calculated using a completely analytical method requiring approximation of the localization of the magnetic fluctuations. By examining the analytical calculation method in detail, the nature and general rules for applications of the method are established.

The accuracy of this method as well as the potential speed and accuracy of a new computer algorithm, the Biased-Selection Monte Carlo method, are demonstrated by reproducing numerically many of the values of certain physical

observables without making the approximation required by the analytical method. The results demonstrate that this new algorithm is accurate and also is reasonable in its consumption of computer time.

The physical observables studied are the static quark potential and the glueball mass of SU(2) Hamiltonian lattice gauge theory. The product of a simple plaquette wavefunction is used as the variational ground state. From the heavy quark potential, the rough transition point is located at $\xi_c = 1/2g_c^2 = 0.26$. The string tension also can be extracted from the heavy quark potential. the string tension exhibits scaling behavior which is consistent with the expected asymptotic scaling line. The scaling behavior of the string tension implies that $\Lambda_H = 0.009\sqrt{\sigma}$, σ being the string tension.

The lowest excited state, including correlations of up to two adjacent plaquettes, is found by using a projection operator to remove the ground state. This enables calculation of the glueball mass. The result exhibits an obvious tendency toward scaling, but the glueball mass in this approximation does not scale exactly along the expected asymptotic scaling line. However, a scaling window is observed in the ratio of glueball mass to the square root of string tension, and it yields

$$M_g = 2.86\sqrt{\sigma} \quad .$$

CHAPTER 1
INTRODUCTION AND OVERVIEW

Quantum chromodynamics (QCD) now is accepted widely as an underlying theory of strong interaction. This theory has two quite different aspects. On one hand, because of the property of asymptotic freedom[1] possessed by the non-abelian gauge theories, at short distance the effective coupling constant of the quark-gluon interaction becomes small. The interaction can then be treated perturbatively and the theory becomes relatively simple. On the other hand, quarks within hadrons are bounded and inseparable. In this situation, the dynamical mechanism becomes very complicated. The complexity can be seen most easily from the fact that the proton is built out of three quarks (u, u and d) which are much lighter than the proton. In order to demonstrate that QCD is a comprehensive theory, the complexity must be overcome and large-scale dynamics must be included.

To this end, lattice gauge theory was introduced by Wilson[2] as a theoretical aid and computation tool to study the large-scale properties of QCD. Once a field theory has been formulated on a lattice, the problem becomes one of statistical mechanica, i.e., reduces in a sense to the evolution of the multidimensional integral known as the partion function. In this work, we used both analytical and Biased-Selection Monte Carlo methods to evaluate this integral at various values of the coupling constant accurately enough to extract information about the physical contents of the system. To understand the

underlying physics, we have to probe the different phases of this system, and understand the nature of its critical points. In particular, if the transition between two different phases of the system is continuous, we can obtain a well defined continuum limit by approaching the critical point of the theory. The phases of the statistical mechanics system can be obtained in a variety of methods, such as duality transformation, high or low temperature expansion, renormalization group technique, etc. For example, the high temperature expansion yields the following form of the two point correlation function of 3-dimension Ising model (3)

$$< S_k S_n > \sim \exp(- mr)$$

as $r = |k - n| \to \infty$, here m is a constant. Using duality transformation, one can show that in the low temperature regime the correlation function above behaves as

$$\Gamma_c = <\prod_c A_\mu> \sim \exp (- \frac{\text{area(c)}}{T})$$

where A_μ are the dual gauge variables, area(c) is the minimal area enclosed by c(a closed curve over the gauge variables on the lattice links), and T is the temperature. Analogously, Wilson introduced the Wilson loop(2) as an order parameter for the nonabelian gauge theories. It is defined as

$$< W(c) > = \mathrm{Tr}\, P \exp\left(i \oint_c A_\mu \, dx^\mu \right) >$$

$$= \int DA \, e^{-S(A)} \, \mathrm{Tr}\, P \exp\left(i \oint_c A_\mu \, dx^\mu \right). \qquad (1\text{-}1)$$

Using perturbative techniques in the weak coupling region, one can show that these nonabelian gauge theories are asymptotically free. In addition, if the above Wilson loop obeys an area law

$$< W(c) > \sim \exp(-\mathrm{area}(c)), \qquad (1\text{-}2)$$

one can show that the theory linearly confines. Since the introduction of lattice gauge theory, many qualitative analyses and numerical simulations have been performed, all of which[4] indicate that the color confinement coexists with asymptotic freedom in QCD, and there is no phase transition between them.

Because the formulation of Euclidean lattice gauge theory preserves reflection positivity and admits a self-adjoint transfer matrix (see Chapter 2), there is also an alternative formalism, the Kogut-Susskind Hamiltonian[5] of SU(N) lattice gauge theory, which is useful in studying the low-lying spectrum of the theory. In this dissertation, all of the analytical calculations and the numerical simulations are done in the Hamiltonian formalism. There is a basic philosophy behind working in the Hamiltonian formulation to deal with a complicated theory such as QCD. For example, consider the relation between the well-analyzed theory of Quantum Electrodynamics (QED) and the

extensively studied phenomena of superconductivity. In principle, it is possible to start from the first principle, QED, and the existence of nuclei and electrons, first to establish the crystal structure of solids, then from that the electron-phonon interaction, then the BCS theory,(6) and finally superconductivity. In practice, however, no one has been able to succeed even in the first step. One need not be overly surprised if one finally has to work in a phenomenological model of hadron physics because of the complexity in QCD. The crucial point of working in the Hamiltonian formalism is to determine the important field configurations which should be included in the wavefunction. The information thus obtained will give a clear physical picture to the large-scale dynamical mechanism of QCD and will provide the necessary ingredients for constructing a phenomenological model, which will go beyond the rather simplified existing models such as the MIT(7) and the SLAC(8) bag models.

To perform calculations in lattice gauge theory, there are two approaches currently used by most of the theorists in the field:

(a) Analytical calculations by the use of strong coupling expansion: In the limit of large lattice spacing, the theory is in a strong coupling region,exhibits confinement, and can be calculated exactly. If there are no phase changes, perturbation theory and the techniques of Padé approximation(9) allow calculations also in the weak coupling region. In this way, small lattice spacing and continuum physics can be reached. This method is widely used both in Lagrangian and Hamiltonian formalisms. However, the success of this approach depends critically on the absence of any phase

transition (including roughening transition), which will prevent the continuation to the weak-coupling regime where the continuum field theory is recovered.

(b) Numerical simulations by the use of Monte Carlo method: With this approach, the Monte Carlo method is applied to the lattice gauge system to evaluate expectation values. The idea of the method is to replace the computation of the expectation value of a quantity θ

$$<\theta> = \frac{\int [\prod_k dU_k] e^{-S[U_k]} \theta}{\int [\prod_k dU_k] e^{-S[U_k]}} \qquad (1\text{-}3)$$

by an average over gauge configurations $\{U\}i$

$$<\theta> = \frac{\sum_i \theta [\{U\}i]}{\sum_i 1} \qquad (1\text{-}4)$$

where the configurations $\{U\}i$ are distributed according to the Boltzmann weight e^{-S}. In the Hamiltonian formalism, $e^{-S[U_k]}$ is replaced by $\psi^2 [U_k]$ where $\psi [U_k]$ is the wavefunction. To replace eq. (1-3) by eq. (1-4), it is necessary to single out the important configurations. This is the technique called "importance sampling."(10) The most well-known and widely used one is the Markov chain.(10) The simple Markov chain has large computer time requirement, and bad error estimates. It is therefore of interest to investigate a

computer algorithm which is potentially more economical in the consumption of computer time and also gives accurate error estimates.

The basic computational method used in this dissertation is the variational method. Starting with a trial wavefunction based on physical properties of the system, calculations are carried out from the strong coupling region down to the scaling region by varying variational parameters as a function of coupling constant. Finally, the result in the scaling region is compared with the expected asymptotic scaling line to determine if the continuum physics is recovered. To carry out this procedure analytically, in Chapter 3.2, a systematic way of performing the calculations motivated by Batrouni's mean plaquette method[11] and Robson's plaquette-space integration[12] is developed. In Chapter 6.2 a new computer algorithm, called the Biased-Selection Monte Carlo method, is introduced. This algorithm was first applied to a hard disk system of statistical mechanics by Coldwell.[13] As a demonstration, the Biased Selection Monte Carlo method is used to estimate some physical quantities. The results indicate that this new algorithm can overcome problems met by other available techniques.

Following the above strategy, using the analytical method developed in Chapter 3 two properties of SU(2) Hamiltonian lattice gauge theory (gluon sector only) are studied in detail in the dissertation: The field configuration of the ground state and the first excited state. For the ground state, the ground state energy per plaquette and static quark potential is studied in Chapter 4; for the first excited state, the glueball mass is studied in Chapter 5. The gauge group SU(2) was studied because of the simplicity of its group structure and yet

similar basic physical contents of SU(3). But, in some ways, the case of SU(2) appears to be more complicated than that of the more realistic gauge group SU(3) because of correlation effects. The results obtained here are helpful in establishing rigorous computational methods, and in understanding the underlying physics.

CHAPTER 2
FORMULATION

In 1974, Wilson [2] introduced an elegant formalism of gauge theories on a space-time lattice. The Minkowskian space-time first is transformed through a Wick rotation into an Euclidian space-time. The Euclidian space-time then is discretized to act as an ultraviolet cut-off, and the theory, which is formulated on a discretized Euclidean space-time lattice, becomes equivalent to a statistical mechanics problem. The most remarkable property of this formalism is that local gauge invariance always remains exact. Besides Wilson's formalism, there is an alternative one, first advocated by Kogut and Susskind.[5] In the Kogut-Susskind Hamiltonian formalism,[5] the time variable is kept continuous and the space variable is discretized. Working in the temporal gauge $A_0 = 0$, they define a Hamiltonian which is a function of the space components of the gauge fields and a set of the conjugate momenta. Instead of being analogous to statistical mechanics in Wilson's formalism, a conventional quantum mechanical system with a well-defined Hamiltonian is dealt with. In Wilson's formalism, strong coupling expansion is analogous to high temperature expansion in statistical mechanics. The Hamiltonian formalism also permits a strong coupling expansion, which is now an application of quantum mechanical perturbation theory.

In this chapter, the Wilson action will be constructed first; then the Kogut-Susskind Hamiltonian will be derived from the Wilson action. Some

discussions and comments are made for both Lagrangian and Hamiltonian formalisms. Finally, the scaling behavior of lattice gauge theory and the continuum physics will be discussed. The information contained in this chapter is not completely new for the researchers in this field. However, here the author has attempted to clear up some clouds ,which once puzzled the author, about the fundamental formulations of lattice gauge theories.

2.1. Lagrangian Lattice Gauge Theory

The action is a mathematical construction with two important properties:

(a) According to the Hamiltonian principle, the classical equations of motion can be obtained by extremizing the action.

(b) According to the Noether theorem, the symmetries of the action correspond to the various conserved quantities in the physical system.

Therefore, a guide for constructing an action is usually the symmetry respected by the physical system. Today, physicists believe that the symmetry associated with the Poincaré group, i.e , the inhomogeneous Lorentz group, is respected by all of the physical systems. In addition, the spectacular results obtained in QED, Quantum Flavordynamics (QFD) and QCD make gauge symmetry indispensable for constructing an action. However, even if the symmetries of the physical system are specified there still are unlimited ways to construct an action. In continuous theory, two properties usually are used to single out a particular action:

(a) Renormalizability, which makes the ultraviolet and the infrared infinities manageable.

(b) Simplicity, as long as the dynamics represented by the action are non-trivial.

The action constructed in this way is called the "minimal action." In lattice formulation of field theory, the space-time symmetry of the Poincaré group is discretized, but an effort is made here to maintain the exact gauge symmetry. Because of the cut-off introduced by the space-time lattice, ultraviolet infinities can be ignored, but the action is constructed to be as simple as possible. This is exactly how the Wilson action is constructed.

2.1.1. The Wilson Action of SU(N) Lattice Gauge Theory

Considering a four-dimensional Euclidean space, a hypercubical lattice with spacing, a, is introduced. Links are defined as the bonds connecting each pair of the nearest neighbor sites. There are eight links emerging from each site. An elementary square, which is enclosed by four links, is called a plaquette. A link pointed from site n along the direction $\hat{\mu}$ to the nearest neighbor site is associated with an independent group element $U_\mu(n)$

$$U_\mu(n) \in SU(N) \quad . \tag{2-1}$$

On transversing a link in the opposite direction, one should obtain the inversed element

$$U_{-\mu}(n + \hat{\mu}) = U_\mu^{-1}(n) \quad . \tag{2-2}$$

The U_μ (n) matrices are defined as

$$U_\mu (n) = \exp(i\, g_o a A_\mu (n + \frac{a}{2}\hat{\mu})) \tag{2-3}$$

where g_o is the bare coupling constant. The vector potential A_μ is the matrix

$$A_\mu = \sum_a A_\mu^a \, T^a \tag{2-4}$$

where T^a are generators of the Lie algebra of gauge group SU(N). The coordinate associated with A_μ should be in the vicinity of the link in question. For convenience, the coordinate is assumed to be in the middle of a given link.

To preserve local gauge invariance, the action should consist of various closed loops. For simplicity, Wilson[2] proposed that the action should be a sum over all plaquettes of the lattice

$$S = \sum_p S_p \tag{2-5}$$

where the subscript P denotes plaquette. The action of each plaquette S_p is the trace of the product of the group elements associated with the four links which form the surface boundaries of the plaquette, as shown in Figure 1.

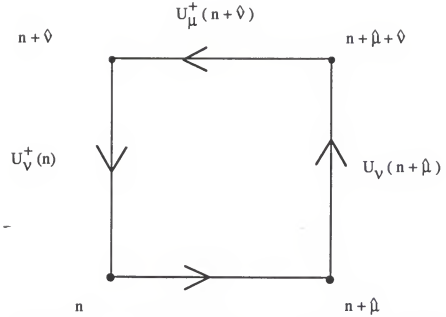

Figure 1. A plaquette Up with $U_p = U_\mu(n)\, U_\nu(n+\hat{\mu})\, U_\mu^+(n+\hat{\nu})\, U_\nu{}^+(n)$

It also is required here that when the group element of a plaquette approaches identity, the action of a plaquette should approach zero. Therefore, the action of a plaquette for the gauge group SU(N) can be written as

$$S_p = \beta\,[1 - \frac{1}{N}\,\mathrm{Retr}\,Up] \tag{2-6}$$

and, for a plaquette laying in the (μ,υ) plane,

$$U_p = U_\mu(n)\, U_\nu(n+\hat{\mu})\, U_\mu^+(n+\hat{\nu})\, U_\nu{}^+(n) \tag{2-7}$$

The normalization factor β will be defined later. The trace in eq. (2-6) can be taken in any representation, but for simplicity only the fundamental representation is considered.

To demonstrate that the action of eq. (2-5) reduces to the usual Yang-Mills theory in the continuum limit, the plaquette-action, eq. (2-6), is expanded with respect to the center position of the plaquette in terms of the powers of lattice spacing, a. Consider, for example, a plaquette lying in the (1,2) plane with the center at n_μ and with counterclockwise orientation. The corresponding action is

$$S_p = \beta \{1 - \frac{1}{N} \mathrm{Re\ tr} [\exp(i g_0 a A_1 (n_\mu - \frac{1}{2} \delta_{\mu,2})]$$

$$\bullet \exp(i g_0 a A_2 (n_\mu + \frac{1}{2} a \delta_{\mu,1}))$$

$$\bullet \exp(-i g_0 a A_1 (n_\mu + \frac{1}{2} a \delta_{\mu,2}))$$

$$\bullet \exp(-i g_0 a A_2 (n_\mu - \frac{1}{2} a \delta_{\mu,1}))]\} \quad . \qquad (2\text{-}8)$$

Taylor expanding the vector potential about the center of the plaquette gives, up to the order $O(a^2)$:

$$S_p = \beta \{1 - \frac{1}{N} \mathrm{Re\ tr} [\exp(i g_o a A_1 (n_\mu) - \frac{i}{2} g_o a^2 \partial_2 A_1 (n_\mu)$$

$$\bullet \exp (i g_o a A_2 (n_\mu) + \frac{i}{2} g_o a^2 \partial_1 A_2 (n_\mu))$$

$$\bullet \exp (-i g_o a A_1 (n_\mu) - \frac{i}{2} g_o a^2 \partial_2 A_1 (n_\mu))$$

$$\bullet \exp (-i g_o a A_2 (n_\mu) + \frac{i}{2} g_o a^2 \partial_1 A_2 (n_\mu))] \} \qquad (2\text{-}9)$$

Use of the Baker-Hausdorff formula

$$\exp (x) \exp (y) = \exp (x + y + \frac{1}{2} [x,y] + ...) \qquad (2\text{-}10)$$

yields

$$S_p = \beta [1 - \frac{1}{N} \mathrm{Re\ Tr} \exp (i g_o a^2 (\partial_1 A_2 - \partial_2 A_1 + i g_o [A_1, A_2]))]$$

$$= \beta [1 - \frac{1}{N} \mathrm{Re\ Tr} \exp (i g_o a^2 F_{12})]$$

$$= \frac{\beta}{2N} g_o^2 a^4 \mathrm{Tr} (F_{12})^2 \qquad (2\text{-}11)$$

Summing over all of the plaquettes gives

$$S = \frac{\beta}{2N} g_o^2 \int d^4 x \frac{1}{2} \mathrm{Tr} (F_{\mu\upsilon})^2 \qquad (2\text{-}12)$$

with the factor of one-half inside the integral coming from the symmetry under $\mu\upsilon$ interchange. If β is defined as

$$\beta = \frac{2N}{g_o^2} \tag{2-13}$$

the Wilson action reduces to the usual Yang-Mills theory in the limit $a \rightarrow 0$.

2.1.2. Discussions and Comments

From the view of constructive quantum field theory, Wilson's lattice formalism of gauge theories has the following properties:

(a) The lattice regularization preserves local gauge invariance: When space-time is discretized, a cut-off is introduced into the theory naturally. The introduced cut-off is proportional to 1/a in momentum space. Usually a cut-off will break local gauge invariance, as in the well-known case of the Pauli-Villars regularization.(14) But as part of the theory, local gauge invariance is necessary in establishing both ultraviolet and infrared properties of the theory. This is exactly the reason that use of the dimensional-regularization(15) in the continuum gauge theories is preferred.

(b) The formulation preserves reflection positivity and admits a self-adjoint transfer matrix:(16) Because of reflection positivity, a positive definite Hilbert space of physical states can be reconstructed; and because of the existence of a self-adjoint transfer matrix, a self-adjoint Hamiltonian also can be defined. These two characteristics guarantee that the formulation specifies an Euclidean quantum field theory.

(c) The formulation reduces to the usual Yang-Mills theory in the limit of lattice spacing approaching zero.

Along with these remarkable properties, there are some problems:

(a) The formulation severely mutilates the space-time symmetry of the Poincaré group: This problem reflects the fact that troubles are encountered in trying to consistently include fermions in the formulation.(17) For the gauge fields, the Lorentz properties appear to be irrelevant to the lattice formulation.

(b) The formulation obscures the topological properties of gauge fields: On a lattice, continuity in space-time is lost and any lattice gauge field $U_\mu(n)$ can be deformed continuously to the trivial field $U_\mu(n) = 1$, where apparently there is no topological structure.

As far as these problems are concerned, it is noted that in the weak-coupling region the space-time symmetry will be restored eventually and gauge fields again will fall into disconnected topological classes. Therefore, topological interpretations can be given to some field configurations according to the topological classes with which they associate in the weak-coupling region. Some work has been done in this direction.(18)

Finally, it is desirable to comment on the Wilson action. In Wilson's action, usually the fundamental representation of a gauge group is used. This is convenient, but there is no natural reason for making this choice. On the other hand, in the previous section it was showed that Wilson's action reduces to the standard Yang-Mills action in the naive continuum limit. The latter property is a necessary requirement for any lattice regularization of the continuum action. However, it is not sufficient to uniquely determine the form of the action.

Therefore it is possible to have various actions, all with the same continuum limit. The question becomes how they approach the continuum limit or, if the action approaches the continuum limit, in a way smooth enough to avoid any artificial phase transition. Based on this consideration, Manton[19] proposed another action which shares many of the properties of the Wilson action. In Manton's approach, the action is constructed in terms of the shortest distance in the group space

$$S_M(U) = \frac{1}{g^2} \sum_p (d(U(p),1))^2 \qquad (2\text{-}14)$$

where d(U(p), 1) denotes the geodesic from U (p) to the unit matrix. The action here is independent of the group representation, and approaches the continuum limits more smoothly than the Wilson action does.[19] Lang et al.[20] used Manton's action to perform calculations for U(N) and SU(N) lattice gauge theories in two dimensions. Their results showed that there is no sign of phase transition at all, even for the $U(\infty)$ theory in which Gross and Witten[21] observed a third-order phase transition by using Wilson's action. However, as stressed by Kogut[22] and others, the detail form of the lattice action should become irrelevant in the continuum limit. While most of the researchers in this field, including this author, still use the Wilson action, it is necessary to be cautious about any transition exhibited by the theory. Monte Carlo studies of the Wilson action show a rapid but smooth crossover from ordered to random behavior for SU(2) and SU(3),[4] and a first-order phase

transition for SU(N) with $N \geq 4$.[23] The last generally is believed to be an artifact of the Wilson action, rather than a transition to a new phase of the continuum theory.[24] Therefore, in regard to SU(2) and SU(3), it is safe to use the Wilson action.

2.2. Hamiltonian Lattice Gauge Theory

The Kogut-Susskind Hamiltonian [5] of SU(N) lattice gauge theory was constructed originally according to the gauge symmetry. In this section for the first time the Hamiltonian is rigorously derived directly from the Wilson action without using the transfer matrix, (using the transfer matrix to derive the Kogut-Susskind Hamiltonian rigorously can be founded in ref.(25)), so that the equivalence can be seen between these two formalisms. To derive the Hamiltonian from the Wilson action, the rules of canonical quantization are followed: The Wilson action first is cast in Hamiltonian form, and then canonical commutation relations between the coordinates and their corresponding conjugate momenta are imposed. Also discussed are the typical problems appearing in the canonical quantization of continuous nonabelian gauge theory[26] and the corresponding status of lattice gauge theory.

2.2.1. Kogut-Susskind Hamiltonian of SU(N) Lattice Gauge Theory

The Wilson action, up to a constant term, is

$$S = \frac{1}{g_o^2} \sum_p \{ \mathrm{tr} U_p + \mathrm{h.c.} \} \qquad (2\text{-}15)$$

Since it is intended to consider the continuous time limit of the Wilson action, the space-time lattice is deformed by introducing different lattice spacings, a and a_o, for space and time. The coupling constants on spacelike plaquettes and timelike plaquettes no longer are equal in the Wilson action

$$S = \frac{1}{g_t^2} \sum_{p_t} \{trU_{p_t} + \text{h.c.}\} + \frac{1}{g_s^2} \sum_{p_s} \{trU_{p_s}^2 + \text{h.c.}\} \tag{2-16}$$

where P_t denotes the timelike plaquette, P_S is the spacelike plaquette, g_S is the bare coupling constant for the spacelike plaquette, and g_t is that for the timelike plaquette. In order to obtain a proper classical limit, g_t^2 and g_s^2 are replaced in eq. (2-16) by

$$\frac{1}{g_t^2} \rightarrow \frac{a}{g_t^2 a_o} \tag{2-17a}$$

and

$$\frac{1}{g_s^2} \rightarrow \frac{a_o}{g_s^2 a} \tag{2-17b}$$

and the Wilson action becomes

$$S = \frac{a}{g_t^2 a_o} \sum_{p_t} \{trU_{p_t} + \text{h.c.}\} + \frac{a_o}{g_s^2 a} \sum_{p_s} \{trU_{p_s} + \text{h.c.}\} . \tag{2-18}$$

In the limit of small lattice spacing, i.e., $a \to 0$ and $a_o \to 0$, we have

$$trU_{p_s} + \text{h.c.} = -g_s^2 a^4 tr(F_{ij})^2 + \text{constant} \tag{2-19a}$$

and

$$trU_{p_t} + \text{h.c.} = -g_t^2 a^2 a_o^2 tr(F_{oi})^2 + \text{constant} \tag{2-19b}$$

Here i,j = 1,2, or 3. Substituting eqs. (2-19a) and (2-19b) into eq. (2-18), a proper classical limit is obtained:

$$S \underset{\substack{a \to 0 \\ a_o \to 0}}{\longrightarrow} \frac{1}{2} \int d^3x\, dt\, Tr\, (F_{\mu\upsilon})^2 \tag{2-20}$$

To proceed toward the Hamiltonian formalism, we now go to the temporal gauge by setting all timelike links equal to identity. The timelike plaquette, as shown in Figure 2, can be written as

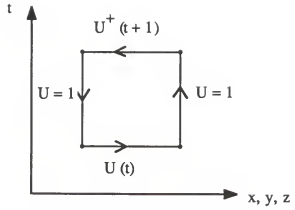

Figure 2. A time-like plaquette in the temporal gauge.

$$\mathrm{tr}U_{p_t} + \text{h.c.} = \mathrm{tr}(U(t)U^{+}(t+1) + \text{h.c.})$$

$$= -\,\mathrm{tr}\{(\,U^{+}(t+1) - U^{+}(t)\,)(\,U(t+1) - U(t)\,)\} + \text{constant} \qquad (2\text{-}21)$$

Substituting eq. (2-21) into eq. (2-18),

$$S = a_o \{ -\frac{a}{g_t^2} \sum_{p_t} \mathrm{tr} \left(\frac{U^{\dagger}(t+1) - U^{\dagger}(t)}{a_o} \bullet \frac{U(t+1) - U(t)}{a_o} \right)$$

$$+ \frac{1}{a g_s^2} \sum_{p_s} \mathrm{tr} \left(U_{p_s} + \text{h.c.} \right) \}$$

$$\xrightarrow[a_o \to o]{} a_o \{ \frac{a}{g_t^2} \sum_{\text{links}} \mathrm{tr}\, \dot{U}^{\dagger} \dot{U} + \frac{1}{a\, g_s^2} \sum_{p_s} \mathrm{tr} \left(U_{p_s} + \text{h.c.} \right) \}. \qquad (2\text{-}22)$$

From eq. (2-22), in the continuum time the Lagrangian of the system can be defined

$$L(t) = \frac{a}{g_t^2} \sum_k \mathrm{tr}\, \dot{U}_k^\dagger \dot{U}_k + \frac{1}{a\, g_s^2} \sum_p (\mathrm{tr}\, U_p + \mathrm{h.c.}) \tag{2-23}$$

where the summations over links and plaquettes only refer to those in three spatial dimensions. The action then is

$$S = \int dt\, L(t) \,. \tag{2-24}$$

Now it is possible to construct the Hamiltonian through the canonical procedure

$$H = \sum_k \{ \dot{U}_k^\dagger \frac{\partial L}{\partial \dot{U}_k^\dagger} + \dot{U}_k \frac{\partial L}{\partial \dot{U}_k} \} - L$$

$$= \frac{a}{g_t^2} \sum_k \mathrm{tr}\, \dot{U}_k^\dagger \dot{U}_k - \frac{1}{a\, g_s^2} \sum_p \mathrm{tr}\, (U_p + \mathrm{h.c.}) \,. \tag{2-25}$$

Note that while working in the temporal gauge, the Lagrangian L(t) and the Hamiltonian H still have the invariance of time-independent local gauge rotation. To quantize the system of eq. (2-25), $\dot{U}_k$ is eliminated in favor of the generators of time-independent local gauge rotation. If an infinitesimal local gauge rotation is made at site n, the resulting transformation is

$$U_k(n) \rightarrow U'_k(n) = U_k(n) + i\,\Sigma^a(n)\,\frac{\tau^a}{2}\,U_k(n) \qquad (2\text{-}26a)$$

However, because links are orientated and

$$U_k^{\dagger}(n) = U_{-k}(n+\hat{k}) \qquad (2\text{-}26b)$$

it also is possible to have the transformation

$$U_{-k}(n) \rightarrow U'_{-k}(n) = U_{-k}(n) - i\,\Sigma^a(n)\,U_{-k}(n)\,\frac{\tau^a}{2} \qquad (2\text{-}26c)$$

The corresponding two sets of generators, $E_k^a(n)$ and $\tilde{E}_k^a(n)$, satisfy

$$[\,E_k^a(n),\,U_j(m)\,] = i\,\frac{\tau^a}{2}\,U_k(n)\,\delta_{j,k}\,\delta_{n,m} \qquad (2\text{-}27a)$$

$$[\,\tilde{E}_k^a(n),\,U_j(m)\,] = -\,U_k(n)\,\frac{\tau^a}{2}\,\delta_{j,k}\,\delta_{n,m} \qquad (2\text{-}27b)$$

$$[\,E_k^a(n),\,E_j^b(m)\,] = i\,f^{abc}\,E_k^c(n)\,\delta_{j,k}\,\delta_{n,m} \qquad (2\text{-}27c)$$

and

$$[\,\tilde{E}_k^a(n),\,\tilde{E}_j^b(m)\,] = i\,f^{abc}\,\tilde{E}_k^c(n)\,\delta_{j,k}\,\delta_{n,m} \qquad (2\text{-}27d)$$

where f^{abc} are structure constants of the gauge group and

$$[\frac{\tau^a}{2}, \frac{\tau^b}{2}] = i f^{abc} \frac{\tau^c}{2} \quad . \tag{2-28}$$

According to the Noether theorem, the generator of the symmetry is

$$E_k^a(n) = \frac{\partial L}{\partial \dot{U}_k(n)} \delta U_k(n) + \frac{\partial L}{\partial \dot{U}_k^+(n)} \delta U_k^+(n)$$

$$= i \frac{a}{g_t^2} \{ tr (\dot{U}_k^+(n) \frac{\tau^a}{2} U_k(n)) - h.c. \} \tag{2-29a}$$

and similarly

$$\tilde{E}_k^a(n) = -i \frac{a}{g_t^2} \{ tr(U_k(n) \frac{\tau^a}{2} U_k(n)) - h.c. \tag{2-29b}$$

By the use of the following identities

$$U^+ U = 1 \qquad \dot{U}^+ U + U^+ \dot{U} = 0 \tag{2-30a}$$

and

$$\sum_{a=1}^{N^2-1} (\tau^a)_{ij} (\tau^a)_{kl} = N \delta_{il} \delta_{jk} - \delta_{ij} \delta_{kl} \qquad (2\text{-}30b)$$

it is possible to compute the quadradic Casmir operator

$$\sum_{a=1}^{N^2-1} E_k^a(n) \; E_k^a(n) = \frac{a^2}{g_t^4} N \, \mathrm{tr} \left(\dot{U}_k^+(n) \, \dot{U}_k(n) \right)$$

$$= \sum_{a=1}^{N^2-1} \dot{E}_k^a(n) \, \dot{E}_k^a(n) \qquad (2\text{-}31)$$

In terms of the Casimir operator, the Hamiltonian becomes

$$H = \frac{g_t^2}{aN} \sum_l \sum_a E_l^a \; E_l^a + \frac{2}{g_s^2} \sum_{aP} (N - \mathrm{Retr\ Up}) \qquad (2\text{-}32)$$

where a constant has been added to the Hamiltonian such that when $U_k = 1$ for all k, $H = 0$. If the geometric mean of g_s and g_t is defined as the bare coupling constant g_H in Hamiltonian formulation

$$g_H^2 = g_s \, g_t \qquad (2\text{-}33)$$

eq. (2-32) becomes the Kogut-Susskind Hamiltonian[5] of SU(N) lattice gauge theory

$$H = \frac{g_t}{g_s} \{ \frac{g_H^2}{aN} \sum_k \sum_a E_k^a E_k^a + \frac{2}{a g_H^2} \sum_p (N - \mathrm{Retr}\, U_p) \} \tag{2-34}$$

Note that the prefactor $\frac{g_t}{g_s}$ approaches unity in the continuous space limit, so this factor can be ignored for spectrum calculations in the continuum.

2.2.2. Discussions and Comments

When the Kogut-Susskind Hamiltonian was derived from the Wilson action in the previous section, the temporal gauge first was specified to start with. But as was mentioned earlier, the Hamiltonian still possesses the invariance of time-independent local gauge rotation. This symmetry is related to the extra degree of freedom in gauge fields. In order to complete the definition of Hamiltonian, it is necessary to eliminate explicitly the unphysical degree of freedom. However, in the continuous nonabelian gauge theory there appear to be some special problems. These problems will be discussed first in the context of continuous nonabelian gauge theory, then in the context of lattice gauge theory.

In the continuous nonabelian gauge theory, the classical Lagrangian density is

$$L = -\frac{1}{4} F^{a\mu\nu} F^a_{\mu\nu} = \frac{1}{4} (\vec{B}^a \cdot \vec{B}^a - \vec{E}^a \cdot \vec{E}^a) \tag{2-35a}$$

where

$$\vec{E}^{\,a} = \vec{\nabla} A^{oa} - \frac{\partial \vec{A}^{\,a}}{\partial t} - g_o f^{abc} \vec{A}^{\,b} A^{oc} \tag{2-35b}$$

and

$$\vec{B}^{\,a} = \vec{\nabla} \times \vec{A}^{\,a} + \frac{1}{2} g_o f^{abc} \vec{A}^{\,b} \times \vec{A}^{\,c} . \tag{2-35c}$$

The equations of motion are

$$\vec{\nabla} \bullet \vec{E}^{\,a} + g_o f^{abc} \vec{A}^{\,b} \bullet \vec{E}^{\,c} = 0 \tag{2-36a}$$

and

$$\vec{\nabla} \times \vec{B} - \frac{\partial \vec{E}^{\,a}}{\partial t} + g_o f^{abc} (A^{bo} \vec{E}^{\,c} + \vec{A}^{\,b} \times \vec{B}^{\,c}) = 0 . \tag{2-36b}$$

To cast the theory in Hamiltonian form, notice that eq. (2-36a) is the nonabelian version of Gauss' law, and A^o is not an independent variable. It can be eliminated through eq. (2-36a) by the use of eq. (2-35b). Therefore it is natural to choose the temporal gauge $A^o = 0$ to case the theory into the Hamiltonian form. The Hamiltonian density is

$$H = \frac{1}{4}(\vec{E}^a \bullet \vec{E}^a + \vec{B}^a \bullet \vec{B}^a) \tag{2-37a}$$

with

$$\vec{E}^a = -\frac{\partial}{\partial t}\vec{A}^a \tag{2-37b}$$

and $\vec{B}^a$ is the same as eq. (2-35c). There are two equations of motion. One gives eq. (2-37b), and the other gives eq. (2-36b). However, Gauss' law, eq. (2-36a), is missing. Therefore it is necessary to impose Gauss' law as a constraint on the Hamiltonian. In general, there are two ways to solve the constraint, and each one has its own difficulty:

a) The constraint is transferred to the gauge condition to impose on the field variables before quantization. Combining eqs. (2-36a) and (2-37b) together, Gauss' law becomes

$$\vec{\nabla} \bullet \frac{\partial \vec{A}^a}{\partial t} + g_o f^{abc} \vec{A}^b \bullet \frac{\partial \vec{A}^c}{\partial t} = 0 \tag{2-38a}$$

Since the structure constant f^{abc} is antisymmetric in b and c

$$g_o f^{abc} \vec{A}^b \bullet \frac{\partial \vec{A}^a}{\partial t} = \frac{1}{2} g_o \frac{\partial}{\partial t}(f^{abc} \vec{A}^b \bullet \vec{A}^c)$$

$$= 0 \tag{2-38b}$$

and Gauss' law becomes

$$\frac{\partial}{\partial t} \vec{\nabla} \bullet \vec{A}^{a} = 0$$

Therefore, imposing the constraint is equivalent to working in the Coulomb gauge

$$\vec{\nabla} \bullet \vec{A}^{a} = 0. \tag{2-39}$$

However, Gauss' law in nonabelian gauge theory is a nonlinear equation, solution to which does not naturally separate $\vec{E}^{a}$ and $\vec{A}^{a}$ into transverse and longitudinal parts to incorporate the Coulomb gauge. It was also pointed out by Gribov[27] that there are ambiguities involved in extracting the dynamical variables in the Coulomb gauge.

b) The constraint is imposed on physical states of Hilbert space: If a state in Hilbert space is represented by Ψ [A] which is in coordinate representation then the Schröedinger operator $\vec{E}(\vec{x})$is represented by

$$\vec{E}(\vec{x}) = i \frac{\delta}{\delta \vec{A}(\vec{x})} \tag{2-40}$$

Under the time-independent gauge transformation

$$\vec{A}^{a}(\vec{x}) \rightarrow \vec{A}^{'a}(\vec{x}) = \vec{A}^{a}(\vec{x}) - \vec{\nabla} \Sigma^{a}(\vec{x}) + g_0 f^{abc} \Sigma^{b}(\vec{x}) \vec{A}^{c}(\vec{x}) \tag{2-41}$$

the wavefunction changes to

$$\psi[\vec{A}^{a}(\vec{x}) - \vec{\nabla}\Sigma^{a}(\vec{x}) + g_0 f^{abc}\Sigma^{b}(\vec{x})\vec{A}^{c}(\vec{x})]$$

$$= \exp\{\int d^3x\,(\vec{\nabla}\Sigma^{a}(\vec{x}) - g_0 f^{abc}\Sigma^{b}(\vec{x})\vec{A}^{c}(\vec{x}))\bullet\frac{\delta}{\delta\vec{A}^{a}(\vec{x})}\}\psi[\vec{A}]$$

$$= \exp\{-i\int d\vec{S}\bullet\vec{E}^{a}(\vec{x})\Sigma^{a}(\vec{x}) + i\int d^3x\,\Sigma^{a}(\vec{x})(\delta^{ac}\vec{\nabla} + g_0 f^{abc}\vec{A}^{b}(\vec{x}))$$

$$\bullet\vec{E}^{c}(\vec{x})\}\psi[\vec{A}]. \qquad (2\text{-}42)$$

If the surface term in eq. (2-42) can be thrown away, the constraint can be satisfied by requiring gauge invariance for physical states in Hilbert space, i.e., if $\psi[\vec{A}'] = \psi[\vec{A}]$,then $\{(\delta^{ac}\vec{\nabla} + g_0 f^{abc}\vec{A}^{b})\bullet\vec{E}^{c}\}\psi[\vec{A}] = 0$ However, because of the non-trivial topological structure of nonabelian gauge fields, the surface term cannot be thrown away. This leads to the famous Θ -vacuum in QCD.(28)

Next to be considered is the situation in lattice gauge theory. The Kogut-Susskind Hamiltonian is symmetric under time-independent local gauge rotation. An operator which performs such transformations can be constructed

$$\Omega[\Sigma(n)] = \exp\{i\sum_{n}\sum_{a}\Sigma^{a}(n)\sum_{k}(E^{a}_{k}(n) + \bar{E}^{a}_{k}(n))\} \qquad (2\text{-}43)$$

Note that by using eq. (2-27) it can be seen that, infinitesimally, the operator Ω does generate the transformation of eq. (2-26). The Hamiltonian, eq. (2-34), commutes with Ω. This follows since the Casimir operator, $\sum_a E^a_k E^a_k$, commutes with all generators of the group. Secondly, the effect of Ω on each link $U_\mu(n)$ is to perform the transformation

$$U_\mu(n) \rightarrow U'_\mu(n) = \exp[i \sum_a E^a(n) \frac{\tau^a}{2}] \, U_\mu(n) \exp[- i \sum_a E^a (n - \hat{\mu}) \frac{\tau^a}{2}] \qquad (2\text{-}44)$$

so the magnetic term of H, $\sum_p$(N-RetrUp), is constructed to be invariant under this transformation. Since

$$[H,\Omega] = 0 \qquad (2\text{-}45)$$

the eigenfunction $\psi[U_k]$ is degenerate with the eigenfunction $\Omega\psi[U_k]$. If it is required that the physical states should be singlet under the transformation of Ω, i.e.,

$$\Omega\psi[U_k] = \psi[U_k] \qquad (2\text{-}46)$$

it implies that

$$\sum_k (E^a_k (n) + \bar{E}^a_k(n)) \, \psi[U_k] = 0 \, . \qquad (2\text{-}47)$$

Using the definitions of $\vec{E}^{a}_{k}(n)$ and $\vec{E}^{a.}_{k}(n)$ in eqs. (2-29a) and 2-29b), it can be shown that in the limit $a \to 0$ eq. (2-47) becomes

$$\{ (\delta^{ac} \vec{\nabla} + g_o f^{abc} \vec{A}^{b}) \bullet \vec{E}^{c} \} \ \psi[\vec{A}] = 0 \ . \qquad (2\text{-}48)$$

Therefore, the constraint of Gauss' law is solved by requiring gauge invariance of the wavefunction. Here there is no difficulty caused by non-trivial topological structure of gauge fields because the topological structure of gauge fields is trivial on the lattice, as discussed in Section 2.1.2.

Finally, two remarks can be made about Hamiltonian formulation:

(a) Since time is kept continuous, it is easier to do numerical simulations in the Hamiltonian formulation because the number of degrees of freedom is reduced. But variables associated with each link are doubled.

(b) The bare coupling constant in Hamiltonian formulation is defined as

$$g^{2}_{H} = g_S \, g_t \, .$$

It is not clear how g_H relates explicitly to the bare coupling constant g_L in Lagrangian formulation. Since the correlation effect depends on the dimensionality of the lattice and higher dimensions imply more correlations, it is therefore expected that for the same physical phenomena, $g_H < g_L$. As will be shown later, this is the case for rough transition in the string tension.

2.3. Continuum Physics and Scaling Behavior

As was mentioned often in the previous sections, the continuum physics will be recovered in the limit of the lattice spacing approaching zero.* However, this does not mean that the continuum physics is reproduced by shrinking the lattice spacing to zero. This is an essential point of lattice gauge calculation. When space-time is discretized, a cut-off is introduced naturally into the theory and the cut-off represents a hidden scale of the theory. Upon renormalization, this hidden scale will be translated to an arbitrary finite scale in the form of a floating renormalization point. If lattice spacing a keeps being reduced and the coupling constant g_0 keeps being renormalized, different but finite scales will appear. Since nonabelian gauge theory is an asymptotic free theory, when a is reduced so that it is sufficiently small then g_0 is weak and the relation between g_0 and a is calculable.

The β- function in Wilson's action can be defined as

$$\beta = a \frac{dg_0(a)}{da} \tag{2-49}$$

In weak region, the perturbative calculation gives

$$\beta(g_0) = \beta_0 g_0^3 + \beta_1 g_0^5 + O(g_0^7) \tag{2-50a}$$

*This section summarizes and somewhat expands a discussion found in ref. (30), it includes a number of results which will be used in the later chapters.

where β_0 for SU(N) gauge theory without fermions is given [1] by

$$\beta_o = (\frac{1}{16\pi^2})(\frac{11N}{3}) \tag{2-50b}$$

to one-loop correction, and β_1 is from a two-loop correction [29] with

$$\beta_1 = (\frac{1}{16\pi^2})^2(\frac{34}{3}N^2) \tag{2-50c}$$

In general, $\beta(g_o)$ depends on the renormalization scheme. However, the first two coefficients in the asymptotic series, β_0 and β_1, are universal. Combining eqs. (2-49) and (2-50) together, we have

$$\frac{dg_o}{\beta_o g_o^3 + \beta_1 g_o^5 + 0(g_o^7)} = d(\log a) \tag{2-51a}$$

Integrating both sides gives

$$\Lambda_L a = (\frac{1}{\beta_0 g_0^2})^{\frac{\beta_1}{2\beta_0^2}} \exp\{-\frac{1}{2\beta_0^2}\} \tag{2-51b}$$

where Λ_L is a constant of integration. Some remarks may be made about this important result, eq. (2-51b):

(a) The result is up to the two-loop correction, and is independent of the renormalization scheme, because β_0 and β_1 are independent of the scheme.

(b) In order to define Λ_L properly, a two-loop correction is needed. The two-loop correction gives the factor before the exponential decrease of the coupling on the right hand side of eq. (2-51b) and in turn gives a proper and finite value of Λ_L.

(c) The value of Λ_L is scheme-dependent and the relation between two Λ_L's can be obtained through a one-loop calculation in perturbation theory.(30) In order to show this, consider two difference schemes each defining a bare coupling as a function of cut-off: $g_0(a)$ and $g'_0(a)$. They must agree with each other in the classical limit

$$g'_0 = g_0 + c\, g_0^3 \tag{2-52}$$

so then

$$\Lambda'_L a = \{ \frac{1}{\beta_0 g'^2_0} \}^{\frac{\beta_1}{2\beta_0^2}} \exp\{ -\frac{1}{2\beta_0 g'^2_0} \}$$

$$\approx \{ \frac{1}{\beta_0 g_0^2} \}^{\frac{\beta_1}{2\beta_0^2}} \exp\{ -\frac{1}{2\beta_0 g_0^2} \} \exp\{ \frac{c}{\beta_0} \} . \tag{2-53}$$

Therefore

$$\log\left(\frac{\Lambda'_L}{\Lambda_L}\right) = \frac{c}{\beta_o} \quad . \tag{2-54}$$

Hasenfratz and Hasenfratz[31] performed the necessary one-loop calculation and found

$$\frac{\Lambda_R}{\Lambda_L} = \begin{cases} 83.5 & \text{For SU(3)} \\ 57.5 & \text{For SU(2)} \end{cases} \tag{2-55}$$

and

$$\frac{\Lambda_H}{\Lambda_L} = \begin{cases} 0.91 & \text{For SU(3)} \\ 0.84 & \text{For SU(2)} \end{cases} \tag{2-56}$$

where Λ_R is calculated in the Feynman gauge for continuous gauge theory, and Λ_H is in the Kogut-Susskind Hamiltonian.

Now consider that a physical quantity, glueball mass M_g for example, is calculated on a lattice. If at a certain range of coupling constant it is observed that the dimensionless quantity $M_g a$ scales with respect to the coupling g_o as

$$M_g a = \text{constant} \bullet \left(\frac{1}{\beta_0 g_0^2}\right)^{\frac{\beta_1}{2\beta_0^2}} \exp\left\{-\frac{1}{2\beta_0 g_0^2}\right\}$$

then the correct continuum physics has been reproduced and an intrinsic scale is set in. In the example here, the constant gives the glueball mass in the unit of intrinsic scale Λ_L. Such a range of go is called the scaling window.

CHAPTER 3
ANALYTICAL CALCULATION METHODS

This chapter is devoted to discussions of analytical methods used in lattice gauge theories and to establishment of a systematic way of calculating the physical observables. As mentioned in Chapter 1, the analytical calculation is usually done by using strong-coupling expansion both in Lagrangian and Hamiltonian formalisms. In Section A, the calculation of string tension is used as an example to discuss the strong-coupling expansion. In the next two chapters, the variational method is used to perform practical calculations in Hamiltonian formalism. To set the stage for later calculations, a systematic way of computing the physical observables analytically in variational calculations is presented in Chapter 2. The method is a combination of Robson's plaquette-space integration[12] and Batrouni's mean plaquette method.[11] Although the discussions of Section B are concentrated to the Hamiltonian formalism, the method also is applicable to calculations in Lagrangian formalism.

3.1. Strong-Coupling Expansion

The strong-coupling expansion is a common and conceptually straightforward way of performing analytical calculations in both Lagrangian and Hamiltonian formalisms, and the results for various physical observables have been obtained by many authors.[22,27,40] As mentioned in Chapter 1, on a

large lattice spacing the theory is in a strong-coupling regime, and the strong-coupling expension technique can be employed. In this section, the expansion of the string tension in the order of the coupling strength is used as an example to discuss the method. The calculations presented here are only carried out to the non-trivial leading order in both the Lagrangian and the Hamiltonian formalisms, and the results are somewhat well known. The purposes of presenting these simple calculations are twofold: One is to show how the linear confinement arises naturally in the lattice gauge theories. Particularly, the physical picture of linear confinement is clearly established in the non-trivial leading order calculation of strong-coupling expansion of the static quark potential in the Hamiltonian formalism. The physical picture thus obtained is helpful for the calculations presented in Chapter 4. Secondly, through the calculation of the string tension, the limitation of the applications of strong coupling expansion can be discussed clearly.

In Lagrangian formalism, the strong coupling expansion is a perturbative expansion in $1/g_0^2$. To obtain the strong-coupling expansion, consider the expectation value of a rectangular Wilson loop of size I • J (Figure 3) in SU(N) lattice gauge theory

$$< W(C) > = \frac{\int [\prod_k dU_k] \left(\frac{1}{N} \mathrm{tr} \prod_{n,\mu \in C} U_\mu(n)\right) \exp\left[\frac{\beta}{2N} \sum_p (\mathrm{tr} U_p + \mathrm{h.c.})\right]}{\int [\prod_k dU_k] \exp\left[\frac{\beta}{2N} \sum_p (\mathrm{tr} U_p + \mathrm{h.c.})\right]} \qquad (3\text{-}1)$$

Here the normalization constant in the action has been cancelled between the numerator and the denominator, and the factor $\frac{1}{N}$ is inserted into the Wilson loop for convenience. Not that the Haar measure $\prod_k dU_k$ is normalized such that

$$\int \prod_k dU_k = 1 \tag{3-2}$$

-Since

$$\int [\prod_k dU_k] U_\mu(n) = 0 \tag{3-3}$$

it is observed that eq. (3-1) vanishes at the zeroth order in β. To go to the first order in β, every link from the action must have a partner, either from the action itself or the Wilson loop. To fill out the Wilson loop with a particular orientation (Figure 4), we should have $I \cdot J$ plaquettes from the action, which then gives the factor $(\frac{\beta}{2N})^{I \cdot J}$. For any two overlapped links in opposite directions

$$\int dU\, U_{ij}\, U^{-1}_{kl} = \frac{1}{N} \delta_{il} \delta_{jk} \tag{3-4}$$

where i, j, k, and l are indices of matrix element. All together, there are $[2I \cdot J + (I + J)]$ links within the Wilson loop, including those in the boundary. The link-integration of eq.(3-4) gives a factor $(\frac{1}{N})^{2I \cdot J + (I + J)}$. After the link integration, the group element associated with each link becomes an identity, and

each trace gives a factor N. In total, there are [I • J + (I + J) + 1] traces within the Wilson loop including the boundary. Therefore, there is another factor, $N^{I \bullet J + (I + J) + 1}$. Combining all of the factors together, the result is

$$< W(C) >_{\beta \to 0}^{\approx} \frac{1}{N} \left(\frac{\beta}{2N}\right)^{I \bullet J} \left(\frac{1}{N}\right)^{2I \bullet J + (I+J)} N^{I \bullet J + (I+J) + 1}$$

$$= \left(\frac{\beta}{2N^2}\right)^{I \bullet J} \qquad \text{for SU(N), N>2.} \qquad (3\text{-}5a)$$

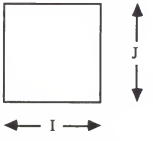

Figure 3. A Wilson loop of size I • J.

Since SU(2) representation is real, it is not necessary to be concerned about the orientation. The factor $\left(\frac{\beta}{2N}\right)^{I \bullet J}$ should be replaced by $\left(\frac{\beta}{N}\right)^{I \bullet J}$, and the result becomes

$$< W(C) >_{\beta \to 0}^{\approx} \left(\frac{\beta}{4}\right)^{I \bullet J} \qquad \text{for SU(2).} \qquad (3\text{-}5b)$$

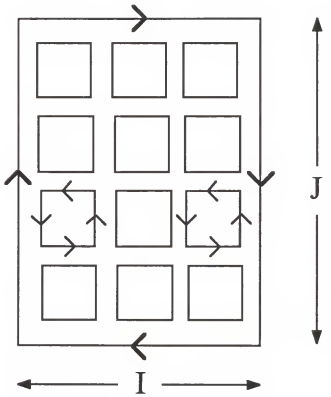

Figure 4. A Wilson loop filled out by plaquettes with proper orientations.

At this non-trivial order of strong-coupling expansion, an area dependence of the Wilson loop has been seen already

$$\langle W(c) \rangle \sim \exp [-\sigma \text{ area } (c)] \qquad (3\text{-}6)$$

where σ is string tension and

$$\sigma a^2 \approx \begin{cases} -\log\left(\frac{\beta}{2N^2}\right) & \text{for SU(N), N>2} \\ -\log\left(\frac{\beta}{4}\right) & \text{for SU(2)} \end{cases} \qquad (3\text{-}7)$$

The procedure can be continued to obtain high order terms in the expansion and then try to extract the continuum physics from the expansion. Before the discussion of continuation, it is important to observe what happens in Hamiltonian formalism.

The quantity in Hamiltonian formalism, related to the Wilson loop in Lagrangian formalism, is the static-quark potential. The area dependence of Wilson loop implies that the static-quark potential is linear to the distance between a pair of quark and antiquark. Therefore, the static-quark potential between a heavy quark at site n and a heavy antiquark at site n + R is considered. To simplify the calculation, the gauge group is specified as SU(2). The Kogut-Susskind Hamiltonian of SU(2) lattice gauge theory is

$$H = \frac{g_H^2}{2a} \sum_k \sum_a E_k^a E_k^a + \frac{2}{a g_H^2} \sum_p (2 - \mathrm{tr} U_p) \qquad (3\text{-}8a)$$

As mentioned in Chapter 2, the Hamiltonian formalism also permits a strong-coupling expansion which is now an application of quantum mechanical

perturbation theory. In the strong-coupling limit, the Hamiltonian of eq.(3-8) is dominated by the color-electric term

$$H_o = \frac{g_H^2}{2a} \sum_k \sum_a E_k^a E_k^a \quad . \tag{3-8b}$$

For each link, it is a quadratic Casimir operator. The corresponding vacuum of eq. (3-8b) thus has each link in a color singlet state

$$E_k^a \mid 0 > = 0 \quad . \tag{3-9}$$

Now consider a heavy $q\bar{q}$ state, a gauge invariant operator is needed to describe the state. The simplest choice of the operator is

$$\Psi^\dagger (n+R) [\prod_{k \in path} U_k] \Psi (n) \mid 0 > \tag{3-10}$$

where the path extends from n to n + R with the minimum number of links required, Ψ (n) is the operator which creats a quark q(n) at site n, and $\Psi^\dagger$ (n+R) creats an antiquark $\bar{q}$(n + R) at site n + R. Note that the color indices are contracted and supressed. For a link there is

$$\sum_a E_k^a E_k^a U_k \mid 0 > = (\sum_a \frac{\tau^a}{2} \bullet \frac{\tau^a}{2}) U_k \mid 0 > = \frac{3}{4} U_k \mid 0 > \qquad (3\text{-}11)$$

where τ^{α}, α = 1, 2 and 3 , are the Pauli matrices. There is, correspondingly, the potential between a quark and an antiquark separated by distance R,

$$V(R) = \frac{g_H^2}{2a} \bullet \frac{3}{4} \bullet \frac{R}{a} = \sigma R \qquad (3\text{-}12)$$

where $\frac{R}{a}$ is the minimum number of links required in the path of eq. (3-10). The string tension then is

$$\sigma a^2 \underset{g_H^2 >> 1}{\rightarrow} \frac{3}{8} g_H^2 \qquad (3\text{-}13)$$

The result obtained here is the leading term in the strong-coupling expansion. In principle, quantum mechanical perturbation theory can be applied to the calculation to obtain higher order terms in the power series of $1/g_H^2$ As stressed in Chapter 2, to extract the continuum physics, the physical observables calculated should exhibit scaling behavior in a certain range of coupling constant. Since the scaling usually happens in the intermediate coupling region, it may be expected that if the higher order terms in the expansion are included the scaling behavior will appear. In the case of string tension, for large enough M it is possible to extract the continuum physics from the expansion

$$\sigma a^2 = f_0 (g_0^2) + \sum_{n=0}^{M} b_n \beta^n \qquad (3\text{-}14)$$

where $\beta = \frac{2N}{g_0^2}$, and $f_0 (g_0^2)$ is equal to $\log (g_0^2)$ in Lagrangian formalism and $\frac{3}{8} g_H^2$ in Hamiltonian formalism. However, in the following two situations the strong-coupling expansion is not sufficient to determine the continuum physics:

(a) If any critical point exists between the strong-coupling and the scaling regions, the expansion coefficients will fluctuate largely, and it is necessary to continue beyond the critical point in the expansion in order to obtain the scaling.

(b) If the scaling region happens at the weak-coupling, or if the symmetry (used to assign the quantum state of the calculated physical observable) can only be restored in the weak-coupling, the expansion will not be able to give the continuum physics.

To save the strong-coupling expansion in these situations, it is possible to employ the Padé approximation [9] when continuing the result of strong-coupling expansion beyond the critical point or going into the weak-coupling region.

The Padé approximation has been studied in statistical mechanics for a long time. The main idea of this approximation is to replace the power series in the expansion by the ratio of two power series

$$\sum_{n=0}^{M} b_n \beta^n = \frac{n_0 + n_1 \beta + \cdots + n_N \beta^N}{d_0 + d_1 \beta + \cdots + d_D \beta^D} \qquad (3\text{-}15a)$$

here $N + D \leq M$. The coeffiecients n_i and d_i are determined by solving the equation

$$(\sum_{i=0}^{D} d_i \beta^i)(\sum_{n=0}^{M} b_n \beta^n) = \sum_{j=0}^{N} n_j \beta^j \qquad (3\text{-}15b)$$

order by order. The critical point corresponds to β_c with

$$\sum_{i=0}^{D} d_i \beta_c^i = 0 \qquad (3\text{-}15c)$$

However, if the system exhibits an unphysical singularity with convergence radius larger than that of the physical one, the straightforward application of the Padé approximation can not give the correct information. It is necessary to make a transformation of the variable β such that the convergence radius is determined by the physical singularity. Unfortunately, this is also the case for the string tension in Lagrangian formalism and it is not known how to transform away the unphysical singularity which is the rough transition point.(33)

From the leading order calculation of the static quark potential, it can be seen that in the strong-coupling region the formation of color-electric flux tubes gives rise to a linear potential between the quarks and supports the confinement phenomena. The quantum effect will set fluctuatation in the flux tube and the transversed width of the flux tube is inversely proportional to the glueball mass. The rough transition of the string tension corresponds to the point where the flux

tube starts to dislocate and continuous translation symmetry is restored effectively. The rough transition here is not a physical singularity because the shape of the flux tube is still maintained even past the transition point.

In the Lagrangian formalism, Monte Carlo results show that the rough transition point exists between the strong-coupling and the scaling regions for SU(2) and SU(3) [4] and, as mentioned in the beginning of this section, it raises serious questions about the continuation of strong-coupling expansion beyond the rough transition point.[29] Our calculation results of Chapter 4 show that a similar situation also appears in the Hamiltonian formalism. Therefore, it also is questionable to use the strong-coupling expansion to calculate the string tension in the Hamiltonian formalism. Considerable effort have been concentrated recently on variational calculations which are able to circumvent these difficulties, since they find the estimates for the physical observables on both sides of these "phase changes."

3.2. Plaquette-Space Integration and Mean - Plaquette Approximation

This section describes the analytical method used to evaluate the integrals necessary for variational calculations. The idea behind variation methods is simple: A trial wavefunction with variational parameters is proposed for a physical state and the parameters then are fixed by minimizing the corresponding energy. The calculations that must be carried out are computations of expectation values of physical observables with respect to the trial wavefunction. Either the Monte Carlo method or the analytical method may be used to perform the calculations. A systematic way of performing the

analytical calculations will be developed in the next section and use of the Monte Carlo method in solving the problem will be the subject of Chapter 6.

3.2.1. Method

In the Lagrangian formalism the Wilson action is

$$S(U_p) = \sum_p \frac{1}{g^2} (\mathrm{tr} U_p + \mathrm{h.c.}) \qquad (3\text{-}16)$$

The ground state expectation value of a physical observable $O(U_p)$ is given by

$$< O(U_p) > = \frac{1}{Z} \int [DU]\, O(U_p) \exp[-S(U_p)] \qquad (3\text{-}16a)$$

where Z is the vacuum to vacuum transition amplitude

$$Z = \int [DU] \exp[-S(U_p)] \qquad (3\text{-}16b)$$

and DU is the Haar measure defined in link space

$$DU = \prod_k dU_k \qquad (3\text{-}16c)$$

which satisfies the left- and right-invariance

$$DU = D(VU) = D(UV) \qquad (3\text{-}16d)$$

where V is an arbitrary element of the SU(N) gauge group. Because the physical observable, $O(U_p)$, is a function of the traces of the various kinds of plaquettes, exists, therefore, is a functional integral in which the integrand is a function of the plaquette and the measure, described in eq. (3-16c), is defined in link space. In 1979, Halpern[34] found a unique inversion for the potential $A_\mu(x)$ in terms of the field strength $F_{\mu\upsilon}(x)$ in continuum gauge theories by using completely fixed axial-like gauge. The variables of the Haar measure therefore can be changed from $A_\mu(x)$ to $F_{\mu\upsilon}(x)$. After fixing the gauge completely, $A_\mu(x)$ has two degrees of freedom, $F_{\mu\upsilon}(x)$ has six degrees of freedom. The constraint is consequently required to be imposed on the field configurations of $F_{\mu\upsilon}(x)$. Halpern[34] showed that the constraint is the Bianchi identities

$$I_\upsilon \equiv D^\mu \tilde{F}_{\mu\upsilon} = 0 \tag{3-17}$$

where $\tilde{F}_{\mu\upsilon} \equiv \frac{1}{2} \in_{\mu\upsilon\alpha\beta} F^{\mu\upsilon}$ is the dual field strength. The Bianchi identities have four components at each space-time point. The constraint therefore reduces the degrees of freedom of $F_{\mu\upsilon}(x)$ to 2. However, not all of the components of the Bianchi identities are independent of each other. Consider a completely fixed axial-like gauge such as

$$A_3(x,y,z,t) = A_1(t,x,y,z_o) = A_2(t,x_o,y,z_o) = A_o(t,x_o,y_o,z_o) = 0 \tag{3-18}$$

where (x_o,y_o,z_o,t_o) is a particular space-time point chosen to start the gauge path. The third component of Bianchi identity is only required at $z = z_o$

$$I_3^a (x,y,z_o,t) = 0. \tag{3-19}$$

Halpern[31] called this the 3 • 1 Bianchi identities. In general,

$$\int [\, DA_\mu \,]\, \delta(\, CFG \,)\, f\,(\, F_{\mu\upsilon} \,)$$

$$= \int [\, DF_{\mu\upsilon} \,]\, \delta[\, I(\, F_{\mu\upsilon}) \,]\, f(\, F_{\mu\upsilon} \,) \tag{3-20}$$

where $\delta(\, CFG \,)$ is the delta-function which imposes the gauge condition, eq. (3-18), and $\delta[\, I(\, F_{\mu\upsilon}) \,]$ is the delta-function for imposing the Bianchi identities to the various field configurations in field-strength space.

Following Halpern's work, Batrouni[11] gave the lattice version of the Bianchi identities as

$$\delta[\, I(\, F_{\mu\upsilon}) \,] \rightarrow \delta(\, P_c - 1 \,) \tag{3-21}$$

By making the gauge transformation $U_p \rightarrow \bar{U}_p$, the lattice Bianchi identity can be abelianized as

$$\delta\,(P_c - 1) \rightarrow \delta\,(\bar{P}_c - 1) = \delta(\prod_{i=1}^{6} \bar{U}_p\,(i) - 1) \tag{3-22}$$

where $\tilde{U}_p(1), \cdots, \tilde{U}_p(6)$ are the six plaquettes which form a cube C and the orientation is assumed to be taken into account properly. However, the gauge degrees of freedom are completely fixed during the course of the unique inversion from U_k to U_p. The question of abelianizing the Bianchi identity is a question of the unique correspondence between a gauge-fixed plaquette and a gauge-invariant plaquette. By constructing explicitly, Batrouni(11) showed that the abelianization can be done over large subspaces of the lattice but will not be complete.

The above arguments can be applied to the Hamiltonian formalism of lattice gauge theories equally well. In the Hamiltonian formalism, the Kogut-Susskind Hamiltonian is obtained from the temporal gauge, and the physical states are subjected to the nonabelian Gauss' law, which implies that the physical states are local gauge invariant. In the coordinate representation, the wavefunction is a function of the traces of the various plaquettes. For a local gauge invariant observable $O(U_p)$, the expectation value with respect to the wavefunction $\psi(U_p)$ is

$$< 0(U_p) > = \frac{\int [DU]\, \psi^+ (U_p)\, 0(U_p)\, \psi(U_p)}{\int [DU]\, \psi^+ (U_p)\, \psi(U_p)} \qquad (3\text{-}23)$$

which is quite similar to eq. (3-16a). To perform the integration of eq. (3-23) in plaquette space, it is possible to choose the completely fixed temporal-like gauge

$$A_o(t,x,y,z) = A_3(t_o,x,y,z) = A_2(t_o,x_o,y,z_o) = A_1(t_o,x,y,z_o) = 0 \quad (3\text{-}24)$$

The temporal-like gauge is compatible with the temporal gauge $A_o(t,x,y,z) = 0$, which is the gauge used to obtain the Kogut-Susskind Hamiltonian. Similar to the Lagrangian formalism, the lattice Bianchi identities must be imposed, and the zeroth component of the Bianchi identities is only required at $t = t_o$

$$I_o^a(x,y,z,t_o) = 0. \quad (3\text{-}25)$$

The difference is in the number of components of the Bianchi identities that must be imposed for a particular plaquette. In the Hamiltonian formalism, the Haar measure is defined in three spatial dimensions. When the measure defined in the link space is converted to that in the plaquette space, the Jacobian is the three spatial components of the Bianchi identities. This is different from the Lagrangian formalism, where the Jacobian is equal to the four components of the Bianchi identities.

Working in plaquette space, as pointed out by Batrouni,(11) the Bianchi identities can be seen as the gradual restoration of strong coupling expansions. For the nonabelian lattice gauge system, it has been demonstrated by various numerical calculations that the confined phase coexists with the non-confined phase, and that the only fixed point is at $g = 0$.(4) Moreover, it has been shown and argued that the vacuum magnetic fluctuations are quite localized.(35) Because of the localization of the magnetic fluctuations in the vacuum, it is

justifiable to work in a local region with the abelianized lattice Bianchi identities while neglecting the nonabelianized identities which usually occur in several lattice spacing units away from the local region. Using the property of localization, Robson[12] was the first to combine the Bianchi identities with character expansion in group representation to establish an analytical calculation method. The essential point of the method is the need for using a small number of the Bianchi identities to obtain the accuracy required. In the following section, Robson's method[12] is modified by combining it with Batrouni's mean-plaquette method[11] and the method is examined in detail for the case of the SU(2) gauge group. The method then may be applied in a straightforward manner to the other gauge group.

The group structure of SU(2) is simple. Since the trace of a plaquette, trU_p, is taken in the fundamental representation, U_p is a two by two matrix and can be parameterized as

$$U_p = \cos(\frac{\rho}{2}) - i\,\vec{n}\bullet\vec{\tau}\,\sin(\frac{\rho}{2}) \tag{3-26}$$

where $\vec{\tau}$ are the Pauli matrixes and $n^a = (\sin\theta\cos\phi,\ \sin\theta\sin\phi,\ \cos\theta)$ is a three dimensional unit vector with $0 \le \rho \le 2\pi$, $0 \le \theta \le 2\pi$, and $0 \le \phi \le 2\pi$. The character of jth representation is denoted as $\chi_j(U_p)$ with

$$\chi_j(U_p) = \sum_{m=-j}^{j} \exp(im\rho) = \frac{\sin[(j+\frac{1}{2})\rho]}{\sin(\frac{\rho}{2})} \tag{3-27a}$$

with $\chi_j(U_p)$ satisfying the orthonormal condition

$$\int dU_p \chi_j(U_p)\chi_k(U_p) = \delta_{j,k} \tag{3-27b}$$

and the product of $\chi_j(U_p)$ can be written as a Clebsch-Gordon series

$$\chi_j(U_p)\chi_k(U_p) = \sum_{m=|j-k|}^{j+k} \chi_m(U_p) \tag{3-27c}$$

From eqs. (3-26) and (3-27a),

$$\mathrm{tr}U_p = \chi_{\frac{1}{2}}(U_p) = 2\cos(\frac{\rho}{2})$$

To simplify the calculation, the product of single plaquette wavefunction is used as the trial ground state wavefunction

$$\Phi_0 = \exp[\lambda \sum_p \mathrm{tr}U_p] = \prod_p \exp[\lambda \mathrm{tr}U_p] \tag{3-28}$$

where λ is a variation parameter. The trial ground state wavefunction is exact in the strong coupling limit and has been shown to be reasonable in the scaling region because of the localization of the magnetic fluctuations in the vacuum. Since Φ_0 is invariant under the transformation

$$U_p \rightarrow V U_p V^+ \tag{3-29}$$

where V is an element of SU(2) gauge group, the abelianized Bianchi identity can be written as a series of separable products

$$\delta(\bar{P}_c - 1) = \sum_{j=0,\frac{1}{2},1,\cdots} \frac{1}{(2j+1)^4} \prod_{i=1}^{6} \chi_j(U_{p_i})$$

$$= 1 + \sum_{j=\frac{1}{2},1,\frac{3}{2},\cdots} \frac{1}{(2j+1)^4} \left[\prod_{i=1}^{6} \chi_j(U_{p_i})\right] \tag{3-30}$$

In principle, the Bianchi identities can be expanded and always yield a series of various integrations effectively in two dimensions. In two dimensions with free boundary condition, the Jacobian of transforming the measure from link space to plaquette space is identity and the integration becomes trivial. For the expectation of plaquette,

$$\langle t_p \rangle \equiv \langle \mathrm{tr}U_p \rangle = \frac{\int dU_p (\mathrm{tr}U_p) \exp(2\lambda\, \mathrm{tr}U_p)}{\int dU_p \exp(2\lambda\, \mathrm{tr}U_p)} = -\frac{1}{\lambda} + 2\frac{I_o(4\lambda)}{I_1(4\lambda)} \tag{3-31a}$$

where $I_n(z)$ is the modified Bessel function defined as

$$I_n(z) = \frac{1}{\pi}\int_0^{\pi} d\theta \cos n\theta \bullet \exp(z\cos\theta) \tag{3-31b}$$

and n is an integer. By continuously differentiating eq. (3-31a) with respect to 2λ, the expectation values of various powers of $\mathrm{tr}U_p$ can be obtained. The results are listed in Table 1. To obtain the expectation value of a plaquette in three dimensions, the Bianchi identities must be inserted to change the measure from link space to plaquette space. In the case of two Bianchi identities (see Figure 5a),

$$< \mathrm{tr}U_p > = \frac{\int [\prod_{i=1}^{11} dU_{p_i}] [\sum_{j_1}\sum_{j_2} \frac{1}{(2j_1+1)^4} \frac{1}{(2j_2+1)^4}}{\int [\prod_{i=1}^{11} dU_{p_i}] [\sum_{j_1}\sum_{j_2} \frac{1}{(2j_1+1)^4} \frac{1}{(2j_2+1)^4}}$$

$$\frac{\chi_{j_1}(U_{p_1})\chi_{j_2}(U_{p_1}) \{\prod_{k=2}^{6} \chi_{j_1}(U_{p_k})\} \{\prod_{n=7}^{11} \chi_{j_2}(U_{p_n})\}]}{\chi_{j_1}(U_{p_1})\chi_{j_2}(U_{p_1}) \{\prod_{k=2}^{6} \chi_{j_1}(U_{p_k})\} \{\prod_{n=7}^{11} \chi_{j_2}(U_{p_n})\}]}$$

$$\frac{[\mathrm{tr}U_{p_1}] \prod_{m=1}^{11} \exp(2\lambda\, \mathrm{tr}U_{p_m})}{\prod_{m=1}^{11} \exp(2\lambda\, \mathrm{tr}U_{p_m})} \qquad (3\text{-}32a)$$

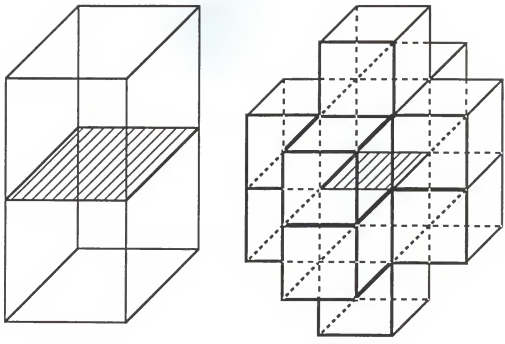

Figure 5. A plaquette
a) with two Bianchi identities; b) with 12 Bianchi identities.

If the numerator and the denominator of the right hand side of eq. (2-21) are both divided by a common factor F

$$F \equiv \int [\prod_{i=1} dU_{p_i}] \prod_{m=1} \exp(2\lambda\, \mathrm{tr} U_{p_m}) \qquad (3\text{-}32b)$$

then both the numerator and the denominator become a power series of the values in Table 1. For a fixed number of Bianchi identities, the convergence in the expansion in j is obtained easily. In the truncation in j the expectation values

of $[\chi_j(U_p)/(2j+1)^{\frac{2}{3}}]$ in two dimensions with $j = \frac{1}{2}, 1, \frac{3}{2}, 2, \cdots$, are measures of the convergence. This quantity vs. the variational parameter λ is plotted in Figure 6.

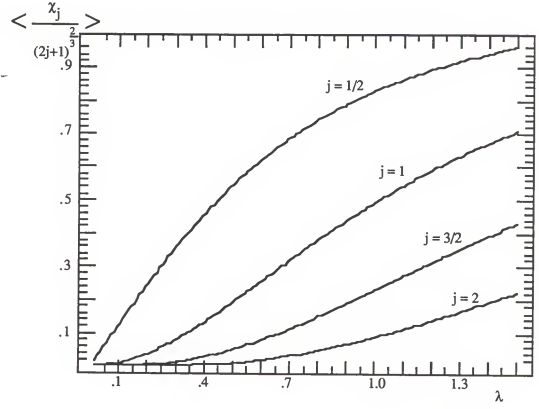

Figure 6. The expectation values of $[\chi_j(U_p)/(2j+1)^{\frac{2}{3}}]$ with j = 1/2, 1, 3/2, 2.

Table 1. The expectation values of various powers of trUp in two dimensions.

Physical Observables	Expectation Values ($t = 4\lambda$)
$\mathrm{tr}U_p = \chi_{\frac{1}{2}}^{1}(U_p)$	$-\frac{4}{t} + 2\frac{I_0(t)}{I_1(t)}$
$\mathrm{tr}^2U_p = \chi_{\frac{1}{2}}^{2}(U_p)$	$(4 + \frac{24}{t^2}) - \frac{12}{t}\frac{I_0(t)}{I_1(t)}$
$\mathrm{tr}^3U_p = \chi_{\frac{1}{2}}^{3}(U_p)$	$-(\frac{40}{t} + \frac{192}{t^3}) + (8 + \frac{96}{t^2})\frac{I_0(t)}{I_1(t)}$
$\mathrm{tr}^4U_p = \chi_{\frac{1}{2}}^{4}(U_p)$	$(16 + \frac{432}{t^2} + \frac{1920}{t^4}) - (\frac{96}{t} + \frac{960}{t^3})\frac{I_0(t)}{I_1(t)}$
$\mathrm{tr}^5U_p = \chi_{\frac{1}{2}}^{5}(U_p)$	$-(\frac{256}{t} + \frac{5376}{t^3} + \frac{23040}{t^5})$ $+ (32 + \frac{1248}{t^2} + \frac{11520}{t^4})\frac{I_0(t)}{I_1(t)}$
$\mathrm{tr}^6U_p = \chi_{\frac{1}{2}}^{6}(U_p)$	$(64 + \frac{4032}{t^2} + \frac{76800}{t^4} + \frac{322560}{t^6})$ $-(\frac{576}{t} + \frac{18240}{t^3} + \frac{161280}{t^5})\frac{I_0(t)}{I_1(t)}$
$\mathrm{tr}^7U_p = \chi_{\frac{1}{2}}^{7}(U_p)$	$-(\frac{1408}{t} + \frac{68736}{t^3} + \frac{1244160}{t^5} + \frac{5160960}{t^7})$ $+ (128 + \frac{10368}{t^2} + \frac{299520}{t^4} + \frac{2580480}{t^6})\frac{I_0(t)}{I_1(t)}$

Table 2. The expectation value of a plaquette with two Bianchi identities

Notations:

$$\langle \mathrm{tr} U_p \rangle_{3D} \equiv \langle \mathrm{tr} U_p \rangle_{2D} \frac{1+N}{1+D}, \quad B \equiv \frac{1+N}{1+D} - 1$$

$$a \equiv \langle \mathrm{tr} U_p \rangle_{2D}, \quad b \equiv \langle \mathrm{tr}^2 U_p \rangle_{2D}, \quad c \equiv \langle \mathrm{tr}^3 U_p \rangle_{2D}$$

$$d \equiv \langle \mathrm{tr}^4 U_p \rangle_{2D}, \quad e \equiv \langle \mathrm{tr}^5 U_p \rangle_{2D}$$

$$N_{\frac{1}{2}} \equiv N(\tfrac{1}{2}, 0) + N(0, \tfrac{1}{2}) + N(\tfrac{1}{2}, \tfrac{1}{2})$$

$$= \frac{1}{8} a^4 b + \frac{1}{256} a^9 c$$

$$N_1 = N(1, 0) + N(0, 1) + N(1, \tfrac{1}{2}) + N(\tfrac{1}{2}, 1) + N(1,1)$$

$$= \frac{2}{81} \frac{1}{a} (c - a) (b - 1)^5 + \frac{1}{648} (d - b) a^4 (b - 1)^5$$

$$+ \frac{1}{6561} \frac{1}{a} (b - 1)^{10} (e - 2c + a)$$

Table 2. Continued

$$D_{\frac{1}{2}} \equiv D(\tfrac{1}{2}, 0) + D(0, \tfrac{1}{2}) + D(\tfrac{1}{2}, \tfrac{1}{2})$$

$$= \frac{1}{8} a^6 + \frac{1}{256} a^{10} b$$

$$D_1 \equiv D(1, 0) + D(0, 1) + D(1, \tfrac{1}{2}) + D(\tfrac{1}{2}, 1) + D(1, 1)$$

$$= \frac{2}{81} (b - 1)^6 + \frac{1}{648} a^5 (b - 1)^5 (c - a)$$

$$+ \frac{1}{6561} \frac{1}{a} (e - 2c + a) (b - 1)^{10}$$

If both Bianchi identities truncate at $j = \frac{1}{2}$, $N = N_{\frac{1}{2}}$, $D = D_{\frac{1}{2}}$.

If both Bianchi identities truncate at $j = 1$, $N = N_{\frac{1}{2}} + N_1$, $D = D_{\frac{1}{2}} + D_1$.

In the figure it is shown that the convergence in j is very fast for small λ (strong coupling region) and slows down for large λ (weak coupling region). To signify the effect of the Bianchi identities, for any physical observables $O(U_p)$ a quantity , B, is defined as

$$\langle O(U_p) \rangle_{3D} = \langle O(U_p) \rangle_{2D} (1 + B) \qquad (3\text{-}33a)$$

so

$$B \equiv \frac{\langle O(U_p) \rangle_{3D} - \langle O(U_p) \rangle_{2D}}{\langle O(U_p) \rangle_{2D}} \qquad (3\text{-}33b)$$

where the subscripts 3D and 2D denote that the expectation value is evaluated in three and two dimensions respectively. Since the quantity B solely represents the effects of the Bianchi identities, the analytical calculation result of the expectation value of any physical observable, $O(U_p)$, can approach to the Monte Carlo calculation result when the number of Bianchi identities is increased in the analytical calculation until the convergence appears in the curve of B vs. λ. The analytical expressions of the expectation value of a plaquette containing two Bianchi identities for the various truncations in j is shown in Table 2. From the curves of B vs. λ in Figure 7, one can see the result of two Bianchi identities converging at j = 1 for λ ranged from 0.05 to 1.1 (or $\frac{1}{2g^2}$ ranged from 0.1 to 0.5).

The next step is to increase the number of Bianchi identities up to 12, where the B vs. λ curve also converges at $j = 1$ for the same range of λ as shown in Figure 8. A comparison between the B-curves of two and 12 Bianchi identities is shown in Figure 9, where there is a non-negligible difference between the two approximations.

To implement this method and more rapidly achieve the convergence, the method can be combined with Batrouni's mean-plaquette method. By replacing the surface plaquettes of the Bianchi identities with the expectation value of these plaquettes,

$$\chi_j(U_p) = U_{2j}(\frac{1}{2}\mathrm{tr}U_p) \rightarrow U_{2j}(\frac{1}{2}<\mathrm{tr}U_p>) \tag{3-34}$$

where $U_{2j}(\frac{1}{2}\mathrm{tr}U_p)$ is the Chebyshev polynomial of the second kind.(36) Similar to the previous procedure, the integration is then done over the internal plaquettes. Note that in order to obtain a consistent result, the number of the Bianchi identities should not be too small. In the following, we will consider two cases: One is the expectation value of plaquette and the other is the expectation value of extended plaquette.

(a) The expectation value of plaquette: Twelve Bianchi identities are used to find the expectation value of plaquette (see Figure 5b). After replacing the surface plaquettes by their expectation values and carrying out the integrations for the internal plaquettes, it yields a polynomial equation

$$P(\lambda) = \frac{\sum_{j_1}\sum_{j_2} \frac{1}{(2j_1+1)^4}\frac{1}{(2j_2+1)^4} M[j_1,j_2,\lambda]\, Q^4[j_1,j_2,\lambda,P(\lambda)]\, R[j_1,j_2,\lambda,P(\lambda)]}{\sum_{j_1}\sum_{j_2} \frac{1}{(2j_1+1)^4}\frac{1}{(2j_2+1)^4} N[j_1,j_2,\lambda]\, Q^4[j_1,j_2,\lambda,P(\lambda)]\, R[j_1,j_2,\lambda,P(\lambda)]} \tag{3-35a}$$

with $P(\lambda) \equiv < trU_p >$, and where

$$N[j_1, j_2, \lambda] = \sum_{j=|j_1-j_2|}^{j_1+j_2} (2j+1)\, I_{2j+1}(4\lambda) \tag{3-35b}$$

$$M(j_1,j_2,\lambda) = \sum_{k=|j_1-j_2|}^{j_1+j_2} \sum_{p=|j-k|}^{j+k} (2j+1)\, I_{2j+1}(4\lambda)\, \delta_{p,\frac{1}{2}} \tag{3-35c}$$

$$Q[j_1,j_2,\lambda,P(\lambda)] = \sum_{j_3}\sum_{j_4} \frac{1}{(2j_3+1)^4}\frac{1}{(2j_4+1)^4} U^4_{2j_3}(\tfrac{1}{2}P(\lambda))\, U^4_{2j_4}(\tfrac{1}{2}P(\lambda))$$

$$N[j_1,j_3,\lambda]\, N[j_2,j_4,\lambda]\, N[j_3,j_4,\lambda] \tag{3-35d}$$

and

$$R[j_1,j_2,\lambda,P(\lambda)] = \sum_{j_3}\sum_{j_4} \frac{1}{(2j_3+1)^4}\frac{1}{(2j_4+1)^4} U^5_{2j_3}(\tfrac{1}{2}P(\lambda))\, U^5_{2j_4}(\tfrac{1}{2}P(\lambda))$$

$$N[j_1,j_3,\lambda]\, N[j_2,j_4,\lambda] \tag{3-35e}$$

The B-curves of the solutions of eq. (2-35a) with different truncations in j are shown in Figure 10, where the curves again converge at j=1 for λ ranging

Table 3. The expectation value of a plaquette.

2λ	analytical calculation	Monte Carlo simulation
0.197(1)	0.195871	0.1964(08)
0.262(1)	0.259291	0.2592(08)
0.326(1)	0.320871	0.3194(08)
0.393(2)	0.384410	0.3848(08)
0.453(2)	0.440293	0.4404(08)
0.516(4)	0.498193	0.4970(10)
0.583(4)	0.558514	0.5572(12)
0.646(3)	0.614177	0.6116(12)
0.699(3)	0.660372	0.6632(12)
0.763(4)	0.715391	0.7140(14)
0.893(8)	0.824369	0.8148(14)
0.996(5)	0.907089	0.9056(16)
1.091(7)	0.980752	0.9810(16)
1.186(7)	1.050616	1.0516(24)
1.385(5)	1.181302	1.1830(10)
1.554(5)	1.272673	1.2770(10)

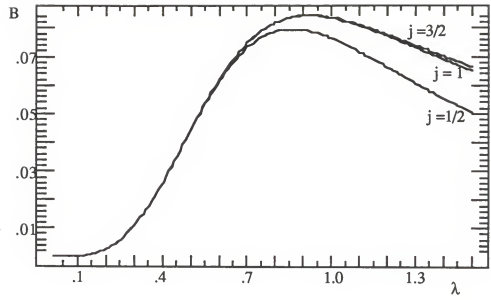

Figure 7. The B-curves of the expectation value of a plaquette with two Bianchi identities and without mean plaquette approximation.

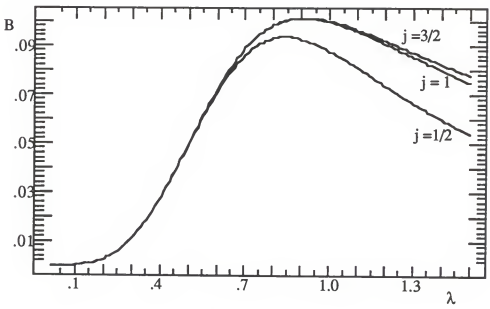

Figure 8. The B-curves of the expectation value of a plaquette with 12 Bianchi identities and without mean plaquette approximation.

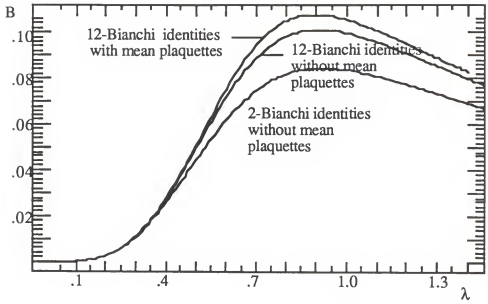

Figure 9. The convergent B-curves of two and 12 Bianchi identities without mean plaquette approximation, and that of 12 Bianchi identities with mean plaquette approximation.

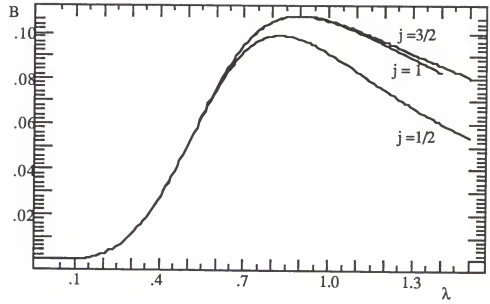

Figure 10. The B-curve of the expectation value of a plaquette with 12 Bianchi identities and with mean plaquette approximation.

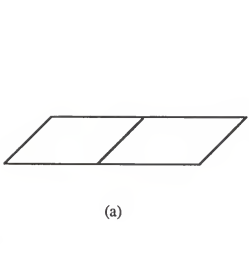

(a)

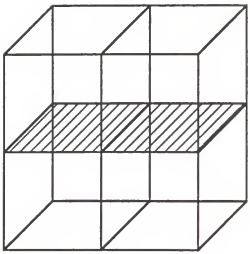

(b)

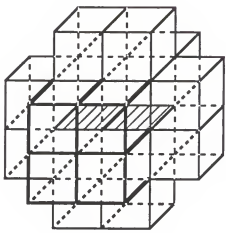

(c)

Figure 11. An extended planar plaquette
a) Without Bianchi identities; b) With four Bianchi identities;
c) With 20 Bianchi identities.

from 0.05 to 1.1. The result of 12 Bianchi identities with the mean plaquette approximation is compared in Figure 9 with the results of two and 12 Bianchi identities without the mean plaquette approximation. Since the largest difference between the results of the 12 Bianchi identities with and without the mean plaquette approximation is 0.004 in B-value for λ ranged from 0.05 to 1.1, the result of the 12 Bianchi identities with mean plaquette approximation can be taken as the convergent result. As shown in Table 3, this result agrees very well with Monte Carlo calculation results, and thus the effect of nonabelianizability of Bianchi identity can be neglected.

(b) The expectation value of an extended plaquette: To calculate the expectation value of an extended planar plaquette which contains two plaquettes (see Figure 11a), the proper Bianchi identities must be built up. Four Bianchi identities can be used to cover the extended plaquette from the top and the bottom (see Figure 11b), then the additional 16 Bianchi identities are used to completely cover the surface of the previous four Bianchi identities (see Figure 11c). Without mean plaquette approximation, the B-curves of the four and the 20 Bianchi identities with different truncations in j are shown in Figure 12 and 13, the curves again converge at j=1 for λ ranging from 0.05 to 1.1. To combine this method with the mean plaquette approximation, each of the surface plaquettes of the Bianchi identities must be replaced by its expectation value, which is the solution of eq. (2-35a). With 20 Bianchi identities, the expectation value is

$$\langle \mathrm{tr}(U_{p_1} U_{p_2}) \rangle = \frac{1}{2} \frac{\sum_{j_1} \sum_{j_2} \sum_{j_3} \sum_{j_4} \left(\prod_{i=1}^{4} \frac{1}{(2j_i+1)^4} \right) M[j_1,j_2,\lambda]\, M[j_3,j_4,\lambda]\, N[j_1,j_3,\lambda]}{\sum_{j_1} \sum_{j_2} \sum_{j_3} \sum_{j_4} \left(\prod_{i=1}^{4} \frac{1}{(2j_i+1)^4} \right) N[j_1,j_2,\lambda]\, N[j_3,j_4,\lambda]\, N[j_1,j_3,\lambda]}$$

$$\frac{N[j_2,j_4,\lambda]\, S^2[j_1,j_2,j_3,j_4,\lambda,P(\lambda)]\, T[j_1,j_2,\lambda,P(\lambda)]\, T[j_3,j_4,\lambda,P(\lambda)]}{N[j_2,j_4,\lambda]\, S^2[j_1,j_2,j_3,j_4,\lambda,P(\lambda)]\, T[j_1,j_2,\lambda,P(\lambda)]\, T[j_3,j_4,\lambda,P(\lambda)]}$$

$$\frac{T[j_1,j_3,\lambda,P(\lambda)]\, T[j_2,j_4,\lambda,P(\lambda)]}{T[j_1,j_3,\lambda,P(\lambda)]\, T[j_2,j_4,\lambda,P(\lambda)]} \qquad (3\text{-}36a)$$

where

$$S[j_1,j_2,j_3,j_4,\lambda,P(\lambda)] = \sum_{k_1} \sum_{k_2} \sum_{k_3} \sum_{k_4} \left(\prod_{i=1}^{4} \frac{U^3_{2k_i}\left(\frac{1}{2}P(\lambda)\right)}{(2k_i+1)^4} \right) N[j_1,k_1,\lambda]$$

$$N[j_2,k_2,\lambda]\, N[j_3,k_3,\lambda]\, N[j_4,k_4,\lambda]\, N[k_1,k_2,\lambda]$$

$$N[k_3,k_4,\lambda]\, N[k_1,k_3,\lambda]\, N[k_2,k_4,\lambda] \qquad (3\text{-}36b)$$

and

$$T[j_1,j_2,\lambda,P(\lambda)] = \sum_{k_1} \sum_{k_2} \left(\prod_{i=1}^{2} \frac{U^4_{2k_i}\left(\frac{1}{2}P(\lambda)\right)}{(2k_i+1)^4} \right) N[j_1,k_1,\lambda]$$

$$N[j_2,k_2,\lambda]\, N[k_1,k_2,\lambda] \qquad (3\text{-}36c)$$

The B-curves of eq. (2-36a) are also convergent at j=1. The convergent B-curve of eq. (2-36a) is compared in figure 14 with the results of four and 20 Bianchi identities without the mean plaquette approximation. Since the difference between the results of 20 Bianchi identities with and without the mean plaquette approximation is so small (0.01 for the largest difference), the result of 20 Bianchi identities with mean plaquette approximation can be taken as the convergent result.

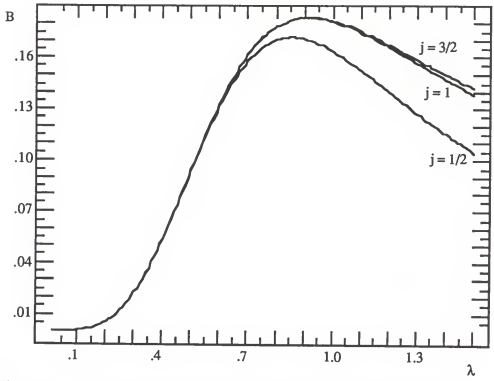

Figure 12. The B-curve of the expectation value of an extended planar plaquette with four Bianchi identities and without mean mean plaquette approximation.

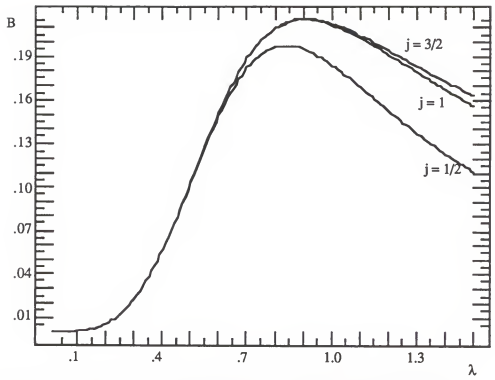

Figure 13. The B-curve of the expectation value of an extended planar plaquette with 20 Bianchi identities and without mean plaquette approximation.

3.2.2 Discussions and Comments

The analytical calculation method presented above is more than simply an alternative calculational method. Rather it reveals insights into the underlying physics and physical structure of the lattice system. For example, from the change in B-curve that occurs as a function of the number of the Bianchi identities, the effect of finite lattice size can be understood explicitly and thus the lattice size needed to avoid the finite-size effect can be estimated. The B-curve also contains some important information about the lattice system and the

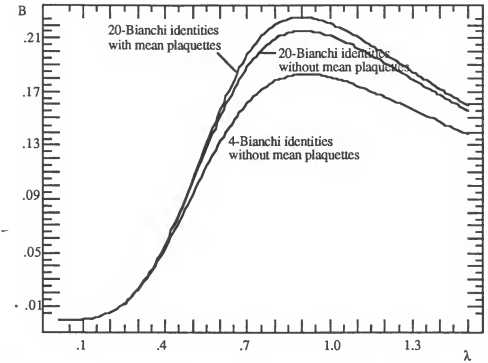

Figure 14. The convergent B-curves of four and 20 Bianchi identities without mean plaquette approximation, and that of 20 Bianchi identities with mean plaquette approximation.

trial wavefunction proposed in the calculation. A typical B-curve of an arbitrary physical observable is shown in Figure 15. The curve can be divided into three regions: One is for $g \geq g_1$, B-value approaching zero, and with the system in the strong coupling region; another is for $g_2 < g < g_1$, B rising rapidly, and with the system in the intermediate coupling region; and the third is for $g \leq g_2$, B-value remaining a constant, and with the system in the weak coupling region. As seen in Figure 9, this is not avoidable for the decline in the B-curve for

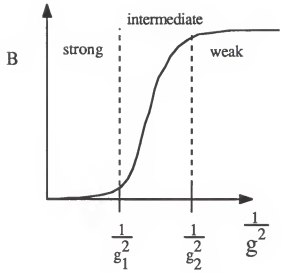

Figure 15. A typical B-curve as a function of coupling constant.

$\lambda > 0.9$ ($\frac{1}{2g^2} > 0.38$) even if the number of the Bianchi identities is increased. This situation indicates that the trial wavefunction proposed is not good enough to incorporate sufficient correlations in the weak coupling region.

Unfortunately, the analytical method presented above is effective only when the trial wavefunction is localized. For example, consider a two-parameter trial wavefunction:

$$\Psi = \exp\{\lambda_1 \sum_{\bar{p}} \mathrm{tr}U_{\bar{p}} + \lambda_2 \sum_{\tilde{p}} \mathrm{tr}U_{\tilde{p}}\} \tag{3-37a}$$

where

$U_{\tilde{p}}$ = the extended plaquette shown in Figure 16(b) (3-37b)

To calculate the expectation value of plaquette, we first evaluate the function

$$f(\lambda_1,\lambda_2) = \frac{1}{N_p} \ln \{ \int [\prod_k dU_k] \exp [2\lambda_1 \sum_p trU_p + 2\lambda_2 \sum_{\bar{p}} trU_{\bar{p}}] \}$$

$$= \frac{1}{N_p} \{ \ln (\int [\prod_k dU_k] \exp [2\lambda_1 \sum_p trU_p])$$

$$+ \ln \left(\frac{\int [\prod_k dU_k] \exp [2\lambda_1 \sum_p trU_p + 2\lambda_2 \sum_{\bar{p}} trU_{\bar{p}}]}{\int [\prod_k dU_k] \exp [2\lambda_2 \sum_{\bar{p}} trU_{\bar{p}}]} \right) \}$$

$$= \frac{1}{N_p} \{ \ln (\int [\prod_k dU_k] \exp [2\lambda_1 \sum_p trU_p]) + \ln < \exp (2\lambda_2 \sum_{\bar{p}} trU_{\bar{p}}) \geq_0 \}$$

$$= \frac{1}{N_p} \{ \ln (\int [\prod_k dU_k] \exp [2\lambda_1 \sum_p trU_p]) + \sum_{n=1}^{\infty} \frac{(2\lambda_2)^n}{n!} < (\sum_{\bar{p}} trU_{\bar{p}})^n \geq_c \}$$

where N_p is the total number of plaquettes; $< V \geq_0$ is the expectation value of physical observables V, obtained by using the wavefunction of eq. (3-37a) with $\lambda_2 = 0$, and $< V^n \geq_c$ stands for the connected part with

$$< V >_c = < V >_0$$

$$< V^n \geq_c = < V^n \geq_0 - < V \geq_0^n \qquad \text{for } n > 1 \tag{3-39b}$$

The expectation value of a plaquette then is

$$< \mathrm{tr} U_p > = \frac{1}{2} \frac{\partial}{\partial \lambda_1} f(\lambda_1, \lambda_2)$$

$$= < \mathrm{tr} U_p \gtrsim_0 + \frac{1}{2N_p} \frac{\partial}{\partial \lambda_1} \{ \sum_{n=1}^{\infty} \frac{(2\lambda_2)^n}{n!} < (\sum_p \mathrm{tr} U_p)^n \gtrsim_c \} \qquad (3\text{-}40)$$

the second term on the right hand side is not easily manageable for $n > 1$ using the analytical method. However, the product of single plaquette wavefunction, eq. (3-28), is exact in the strong coupling region and the scaling region for SU(2) gauge theory is in the range of $0.25 \lesssim \frac{1}{2g^2} \lesssim 0.3$ ($0.3 \lesssim \lambda \lesssim 0.7$), it is thus reasonable to use eq. (3-28) as the trial ground state to carry out the calculation down to the scaling region. Whether or not the continuum physics can be extracted from the calculation, it is necessary to check if the result obeys the scaling behavior as discussed in Chapter 2.3.

To conclude this section, final points should be noted:

(a) From the two examples of calculations worked out here, a general rule for building-up a sufficient number of Bianchi identities can be developed. For a physical observable which is a function of plaquettes, enough Bianchi identities first must be used to cover completely the considered plaquettes from top and bottom. Then additional Bianchi identities are used to cover completely the surface plaquettes of the previous Bianchi identities. To perform the

calculation, the surface plaquettes of the whole Bianchi identities established are replaced by the mean plaquette and all of the Bianchi identities are truncated at j=1. This general rule will be applied in carrying out the calculations that follow.

(b) Considering both planar- and a nonplanar-extended plaquettes (see Figure 16), one Bianchi identity is needed to correlate two plaquettes in a nonplanar-extended plaquette and two Bianchi identities are needed for the case of a planar-extended plaquette. By using four Bianchi identities, the B-curves of the expectation values of these two quantities are shown in Figure 17. From the B-curves it is possible to see that the effect of the Bianchi identities on the nonplanar case is larger than the effect on the planar case. In a similar manner, one can determine the most probable configuration for the collective mode which is crucial in the study of the glueball mass.

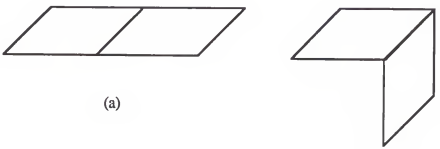

Figure 16. The extended plaquettes
a) Planar; b) Non-planar.

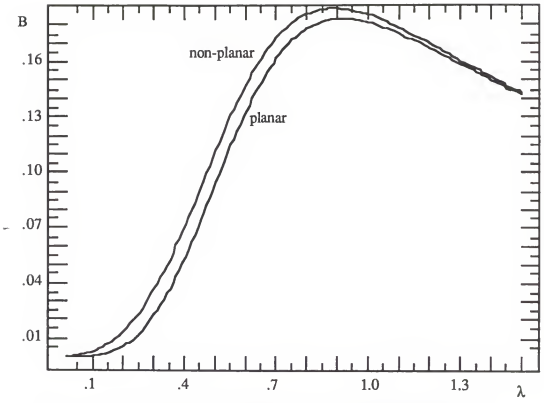

Figure 17. The B-curves of the expectation values of a planar- and a nonplanar-extended plaquette with four Bianchi identities.

CHAPTER 4
VARIATIONAL VACUUM AND STATIC QUARK POTENTIAL FOR SU(2) HAMILTONIAN LATTICE GAUGE THEORY

The calculation of the vacuum energy is most natural in the Hamiltonian formalism since the vacuum energy is the ground state expectation value of the lattice Hamiltonian

$$E_0 = \frac{\langle \Psi_0 | H | \Psi_0 \rangle}{\langle \Psi_0 | \Psi_0 \rangle}$$

The vacuum energy is not a physical quantity. However, the difference between the vacuum energy density in the strong- and the weak-coupling limits may have some physical implications since this is just the "Bag" constant in the M.I.T. Bag model [7] of hadrons. The crucial step in any variational calculation is to propose a reasonable trial ground state wavefunction that is capable of describing the vacuum properties. This will be the subject of Section 1.

The static quark potential is a physical quantity which is related to the vacuum structure. Introducing a quark-antiquark pair into the vacuum, accomplished in Chapter 2, permits study of the static quark potential which is defined as the energy difference between the vacuums with and without the fermion pair.

4.1. Ground State Energy per Plaquette

The Kogut-Susskind Hamiltonian is

$$aH = \frac{1}{4\xi} \sum_k \sum_a E_k^a + 4\xi \sum_p [2 - \mathrm{tr} U_p] \tag{4-1a}$$

where $\xi = \frac{1}{2g^2}$, and the E_κ^a are the color-electric field operators which satisfy the commutation relation

$$[\, E_{k'}^a \;\; U_{k'} \,] = \delta_{kk'} \frac{\tau^a}{2} U_k$$

where τ^a are the Pauli matrices. The trial ground state wavefunction used is

$$\Psi_o = \exp\{\lambda \sum_p \mathrm{tr} U_p\} \tag{4-2}$$

where λ is a variational parameter. As discussed in Chapter 3.2.2, this trial wavefunction is exact in the strong-coupling limit, and it is a reasonable approximation in the intermediate region. Using integration by parts, it can be shown[37] that

$$< \Psi_o \,|\, \sum_a \sum_a E_k^a E_k^a \,|\, \Psi_0 > = \frac{1}{2} < \Psi_0 \,|\, \sum_k \sum_a [\, E_k^a , [\, E_k^a , \ln \Psi_0 \,]] \,|\, \Psi_0 > \tag{4-3a}$$

Thus, the kinetic energy is

$$\frac{\langle \Psi_0 | \sum_k \sum_a E_k^a E_k^a | \Psi_0 \rangle}{\langle \Psi_0 | \Psi_0 \rangle} = \frac{3}{2} \lambda N_p P(\lambda) \tag{4-3b}$$

where N_p is the total number of plaquettes and

$$P(\lambda) = \frac{1}{N_p} \frac{\langle \Psi_0 | \sum_p \mathrm{tr} U_p | \Psi_0 \rangle}{\langle \Psi_0 | \Psi_0 \rangle} \tag{4-3c}$$

is the expectation value of a plaquette. The ground state energy per plaquette is

$$a\mathcal{E}_0 = \frac{1}{N_p} \frac{\langle \Psi_0 | a H | \Psi_0 \rangle}{\langle \Psi_0 | \Psi_0 \rangle} = \left(\frac{3\lambda}{8\xi} - 4\xi \right) P(\lambda) + 8\xi \tag{4-4a}$$

and the variational parameter λ is determined by minimizing $a\mathcal{E}_o$ with respect to λ, which gives

$$\xi^2 = \frac{3}{128} \left[\frac{P(\lambda)}{4P'(\lambda)} + 4\lambda \right] \tag{4-4b}$$

where $P'(\lambda)$ is the derivative of $P(\lambda)$ with respect to λ. Therefore, to find the ground state energy per plaquette, the quantity that must be calculated is the expectation value of a plaquette. Using the result obtained in Chapter 3.2.1,

where the expectation value of a plaquette is calculated by using 12 Bianchi identities with mean plaquette approximation, the resultant ground state energy per plaquette is shown in Figure 18.

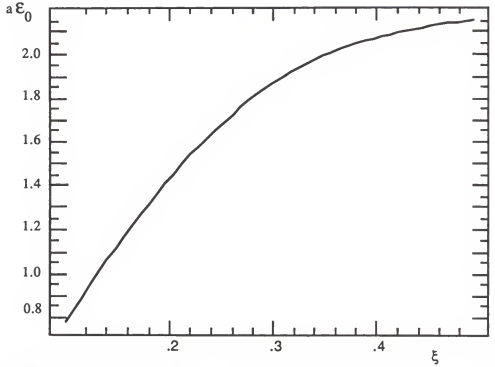

Figure 18. The ground state energy per plaquette as a function of coupling constant.

The exact ground state energy per plaquette also can be obtained through numerical computation. The utility of applying stochastic techniques developed for quantum many-body systems to the study of Hamiltonian lattice gauge theory has been demonstrated. Chin et al.[38] applied the guided-random walk algorithm to solving the ground state energy of the SU(2) lattice gauge theory.

In Table 4, our result for the ground state energy per plaquette is compared with the Monte Carlo calculations. The second column in Table 4 displays Chin et. al.'s Monte Carlo result[38] using the variational ground state eq. (4-2). As can be seen our analytical calculation agrees very well with the Monte Carlo calculation. The third column in Table 4 provides the exact results obtained by Chin et. al.,[38] the difference between the variation results and the exact ones appear only after the second decimal for the scaling region, which is about the range of $0.25 \leq \frac{1}{2g^2} \leq 0.3$. It therefore can be seen that the vacuum fluctuation is quite localized and that the magnetic fluctuations are unlikely to correlate plaquettes separated by more than one unit of lattice spacing for the intermediate coupling region. If the magnetic fluctuations of two units of lattice spacing can be included in the trial ground state, the difference between the variational results and the exact ones will be reduced for the intermediate coupling region. However, because of the complexity involved in eq. (3-40), eq. (4-2) will be used as the trial ground state to perform analytical calculations for the static quark potential and the glueball mass of SU(2) Hamiltonian lattice gauge theory.

4.2. Static Quark Potential

To give a clear global physical picture to the lattice calculation of the static quark potential, a simple model is presented in the first part of the section. The model is that of a rigid vacuum with fluctuating string, which originally was constructed by Lüscher.(39) In the second part, the analytical method

Table 4. The variational and exact ground state energies per plaquette.

$\xi = \frac{1}{2g^2}$	$2\xi_s a E_0$		
	analytical and variational	Monte Carlo and variational	exact
0.136(9)	0.28510093	0.28510(001)	0.28510(006)
0.158(1)	0.37362619	0.37365(001)	0.37356(011)
0.176(8)	0.45902315	0.45903(002)	0.45872(006)
0.193(6)	0.54136152	0.54136(002)	0.54050(009)
0.209(2)	0.62072482	0.62073(004)	0.61943(011)
0.223(6)	0.69720007	0.69727(006)	0.69527(013)
0.237(2)	0.77085766	0.77079(005)	0.76742(022)
0.25	0.84176066	0.84171(007)	0.83581(028)
0.262(2)	0.90997328	0.90989(008)	0.90231(032)
0.273(9)	0.97556613	0.97560(010)	0.96682(042)
0.295(8)	1.09917318	1.09913(020)	1.08357(064)
0.316(2)	1.21321877	1.21305(023)	1.18809(058)
0.335(4)	1.31859769	1.31875(020)	1.28321(083)
0.353(6)	1.41637802	1.41688(028)	1.37865(102)
0.395(3)	1.63488530	1.63615(033)	1.57650(079)
0.433(0)	1.82695077	1.82586(070)	1.76400(112)

developed is used to calculate the static quark potential. Using the static quark potential as a function of the separation distance between quark and antiquark, the critical coupling strength for the restoration of rotational symmetry is located and the string tension is extracted by fitting the potential to a simple polynomial of the separation distance. Finally, the scaling behavior of string tension is examined by comparing this behavior with the expected asymptotic scaling line.

4.2.1. Simple Model for Static Quark Potential: Rigid Vacuum with a Fluctuating String

From the simple calculation using strong-coupling expansion in Chapter 3.1, one can see that the chromoelectric flux tube is formed in the strong coupling limit. Because of the potential energy term, $\frac{1}{2g^2} \sum_p [2 - \mathrm{tr}U_p]$, the flux tube starts to fluctuate when the coupling strength decreases. On the other hand, it was demonstrated that the magnetic fluctuations in the vacuum are quite localized. Combining these two facts, we assume that the vacuum is rigid, and in the presence of a static quark-antiquark pair at a finite distance, L, the glue field can be described by a fluctuating thin tube containing the chromoelectric flux which flows from the quark to the antiquark. Since interest here is only in the low-momentum mode, the degrees of freedom inside the flux tube are not disturbed. Thus, the dynamics of a relativistic thin string can be considered, and the result is independent of the gauge group.

Supposing that the quarks are located at $\vec{x} = (0, 0, 0)$ and $\vec{x} = (L, 0, 0)$, the string then can be described by a two-component vector field

$\vec{\xi}(x^0, x^1),\ 0 \le x^1 \le L$, with $\vec{\xi}(x^0, 0) = \vec{\xi}(x^0, L)$

as shown in Figure 19. To study the dynamics of a thin string, the effective

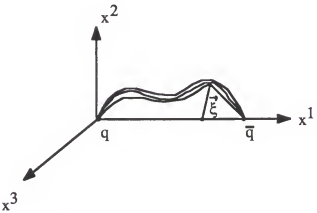

Figure 19. The $\vec{\xi}$-field.defined in the dynamics of a thin string.

action for the $\vec{\xi}$-field. must be known. As discussed in the beginning of Chapter 2, the symmetry manifested by the system is the most plausible guideline for constructing the action. Therefore, the action can be expected to have the following general properties:

(a) the effective action must be local, i.e.

$$S_{eff} = \int_{0 \le x^1 \le L} dt\, dx^1\, L(x) \tag{4-5}$$

where the Lagrangian density, L(x), depends on the $\vec{\xi}$-field. and its derivative.

(b) L(x) should be invariant under the following symmetry operations:

(i) Pointcare transformation in the (x^0, x^1) plane ;

(ii) O(2) rotations and translation of the $\vec{\xi}$ field.

The property (b-ii) precludes mass term $\vec{\xi}(x) \bullet \vec{\xi}(x)$ in the Lagrangian density. The string thus is massless and L(x) must be made up of derivatives

$$\partial_\mu \vec{\xi}, \partial_\mu \partial_\upsilon \vec{\xi}, \cdots, (\mu, \upsilon = 0, 1).$$

So as a result

$$S_{eff} = \int_{0 \le x^1 \le L} dx^0 dx^1 \{ \partial_\mu \vec{\xi} \bullet \partial^\mu \vec{\xi} + b (\partial_\mu \partial^\upsilon \vec{\xi}) \bullet (\partial_\upsilon \partial^\mu \vec{\xi})$$

$$+ c (\partial_\mu \partial^\mu \vec{\xi})^2 + \cdots \} \qquad (4\text{-}6)$$

The effective action, eq. (4-6), is not renormalizable and the parameters b and c are dimensional. However, only the low-momentum mode, where the wavelength is much longer than the intrinsic width of the string, is of interest here. For the high-momentum mode, the internal degrees of freedom of the tube are excited, and the physical picture expressed by the fluctuating string breaks down. Therefore, those terms with dimensional parameters are irrelevant to low-energy physics and it is sufficient to take

$$S_{eff} = \int_{0 \le x^1 \le L} dx^0\, dx^1 \{ \partial_\mu \vec{\xi} \cdot \partial^\mu \vec{\xi} \} \tag{4-7}$$

as the effective action. There are two important features of this action:

(a) The roughening effect from the fluctuation in the string: Because the $\vec{\xi}$ - field is massless, the variance in $\vec{\xi}(x_o, x^1)$ for any x^1 between 0 and L is

$$< \vec{\xi}^{\,2} (x^o, x^1) > \sim \int \frac{d^2k}{k} \sim \ln \left(\frac{L}{a}\right) \tag{4-8}$$

where a is the intrinsic width of the tube. Since the variance is proportional to $\ln(\frac{L}{a})$, an infinitely long localized flux tube cannot exist in a continuum Yang-Mills theory. In lattice gauge theories, the situation is quite different. In this case, the translational symmetry is only discrete. Consequently, there is a mass gap which is proportional to g^2, separating the excited mode and the ground state. For a coupling strength just below the critical value g_c^2, the mass gap becomes easy to overcome, the flux tube appears rough, and the bulk rotational symmetry is restored.

(b) The correction to linear confinement: Because of the zero-mass fluctuation of the string, there are power corrections to the linear quark potential

$$V(L) = \sigma L + \frac{\alpha}{L} + \frac{\beta}{L^2} + O(L^3) \tag{4-9}$$

where σ is the string tension, α is a dimensionless parameter, and β is a parameter with dimension of length. The $\frac{1}{L}$ term is due to a one-dimensional Casimir effect[22] and the coefficient is universal

$$\alpha = -\frac{\pi}{12} \approx -0.26$$

where the minus sign implies the force is attractive. In the lattice gauge theories, because of the existence of the mass gap, eq. (4-9) is modified as

$$V(L) = \sigma L + \frac{\delta}{a} + \frac{\alpha}{L} + O(L^{-2}) \qquad (4\text{-}10)$$

where the constant δ is dimensionless and corresponds to the mass gap between the ground state and first excited state of the flux tube. The string tension σ has dimension of mass squared and is a function of coupling constant. In the next section, σ will be determined by calculating V(L) at various values of L and coupling constant g_0 .

4.2.2. Static Quark Potential for SU(2) Hamiltonian Lattice Gauge Theory

In this section where the static quark potential,* is calculated, it is necessary to impose a quark-antiquark pair into the vacuum. Consider a

*For the calculation of the static quark potential in two spatial dimensions, see ref. (40).

$\bar{q}q$ state, where q and $\bar{q}$ denote a heavy quark-antiquark pair, respectively: Let q and $\bar{q}$ be created by the operators $\Psi(\vec{n})$ and $\Psi^{+}(\vec{n})$. The generator of a color rotation, which was defined in eq.(2-27), now is generalized to

$$\sum_k E^a_k(\vec{n}) \rightarrow \sum_k E^a_k(\vec{n}) + \Psi^{+}(\vec{n}) \frac{\tau^a}{2} \Psi(\vec{n}) \tag{4-10}$$

at site $\vec{n}$. To describe the heavy $\bar{q}q$ state , one should choose an operator which is invariant under the transformation (4-10). The operator

$$\Psi^{+}(\vec{n}) \{ \prod_{k \in path} U_k \} \Psi(\vec{n} + \vec{R}) \tag{4-11a}$$

where the path extends from $\vec{n}$ to $\vec{n} + \vec{R}$ but otherwise is arbitrary, satisfies this requirement. Combining the operator, eq. (4-11a), with the vacuum obtained in Section 4.1 of this chapter, the $\bar{q}q$ state in the gluon field background is described by

$$\Psi^{+}(\vec{n}) \{ \prod_{k \in path} U_k \} \Psi(\vec{n} + \vec{R}) | \psi_0 > \tag{4-11b}$$

where $| \psi_0 >$ is the variational vacuum defined in eq. (4-2). Note that the vacuum of eq. (4-11a) is rigid and independent of the coupling strength. In the strong-coupling region, there is no significant difference between eqs. (4-11a) and (4-11b) because the variational vacuum is almost rigid, i.e. the variational parameter λ of eq. (4-2) is small in the strong coupling region. But the

difference is significant in the intermediate region where localized magnetic fluctuations exist in the variational vacuum.

For a quark and antiquark pair, the quark is placed at the origin and the antiquark is at lattice site (n_x,n_y,n_z). In general, there are infinite ways to choose a path to go from the origin to the lattice site (n_x,n_y,n_z). The dimension of the Hilbert space spent by the states of eq. (4-11b) thus is infinite. To pick up a subset of the Hilbert space, the following two important simplifications are made:

(a) The paths chosen in eq. (4-11b) are those which possess the shortest distance from the origin to the lattice site (n_x,n_y,n_z). The states thus defined in eq. (4-11b) give the lowest energy in the leading order of strong-coupling expansion.

(b) To further reduce the number of states, the antiquark is always placed in the x-y plane.

After these two simplifications, each path in eq. (4-11b) contains the (n_x+n_y) links, and the dimension of this subset is $\frac{(n_x+n_y)!}{n_x!\,n_y!}$ for a particular set of nx and ny.

After choosing the subspace, the next step is to compute the matrix elements of the Hamiltonian with respect to the states in the subset. Let the ith state be

$$| i > = \Psi^{+}(n_x, n_y) F_i \Psi(0, 0) | \psi_0 > \tag{4-12a}$$

and

$$F_i = \prod_{k \in \text{path } i} U_k \tag{4-12b}$$

where U_k is given in eq.(2-3). The contribution from the magnetic potential to the matrix element of the Hamiltonian between states $| i >$ and $| j >$ is

$$\frac{< i | \sum_p (2 - \text{tr}U_p) | j >}{<\psi_0 | \psi_0>} = 2N_p < \text{tr} (F_i^{+} F_j) > - \frac{1}{2} \frac{\partial}{\partial \lambda} < \text{tr} (F_i^{+} F_j) >$$

$$- < \sum_p \text{tr}U_p > < \text{tr} (F_i^{+} F_j) >$$

$$= < \sum_p (2 - \text{tr}U_p) > < \text{tr} (F_i^{+} F_j) > - \frac{1}{2} \frac{\partial}{\partial \lambda} < \text{tr} (F_i^{+} F_j) > \tag{4-13}$$

The left hand side of eq. (4-13) is divided by $<\psi_0 | \psi_0>$ for convenience and the expectation values on the right hand side are evaluated with respect to the variational vacuum $| \psi_0 >$ in eq. (4-2). The contribution from the chromo-electric term in the Hamiltonian is

$$\frac{<i|\sum_k^a E_k^a E_k^a|j>}{<\psi_0|\psi_0>} = \frac{3}{2}\lambda\{\frac{1}{2}\frac{\partial}{\partial\lambda}<tr(F_i^+F_j)> + <\sum_p trU_p><tr(F_i^+F_j)>$$

$$+\frac{3}{8}(n_x+n_y+C_{ij}(n_x,n_y))<tr(F_i^+F_j)> \quad (4\text{-}14)$$

where $C_{ij}(n_x,n_y)$ is the number of common links between Fi and Fj. The derivation of eq. (4-14) is shown in Appendix A. Combining eqs. (4-13) and (4-14) yields

$$\frac{<i|aH|j>}{<\psi_0|\psi_0>} = N_p(\frac{3\lambda}{8\xi} - 4\xi)P(\lambda)<tr(F_i^+F_j)>$$

$$+(\frac{3\lambda}{16\xi} - 2\xi)\frac{\partial}{\partial\lambda}<tr(F_i^+F_j)>$$

$$+\frac{3}{32\xi}[n_x+n_y+C_{ij}(n_x,n_y)]<tr(F_i^+F_j)> \quad (4\text{-}15)$$

where the first term on the right hand side of eq. (4-15) is simply the contribution from the vacuum energy defined in eq. (4-4a). Therefore, the matrix element of the static quark potential between states $|i>$ and $|j>$ is

$$V_{ij}(n_x,n_y) = +(\frac{3\lambda}{16\xi} - 2\xi)\frac{\partial}{\partial\lambda}<tr(F_i^+F_j)>$$

$$+\frac{3}{32\xi}[n_x+n_y+C_{ij}(n_x,n_y)]<tr(F_i^+F_j)> \quad (4\text{-}16)$$

Since the states which belong to the chosen subset are not orthogonal to each other

$$M_{ij} \equiv \frac{<i|j>}{<\psi_0|\psi_0>} = <tr(F_i^+ F_j)> \tag{4-17}$$

As a result, it is necessary to diagonalize the matrix M to form a set of orthogonal states and then to normalize each state. This is just the Schmidt orthogonalization process and the process yields a set of orthogonal states $\{|k>\}$ with

$$|k> = (S D^{-\frac{1}{2}})_{ki} |i> \tag{4-18}$$

where S is the transformation which diagonalizes the matrix M,

$$S^+ M S = D \tag{4-19}$$

D is a diagonal matrix, and $D^{-\frac{1}{2}}$ also is a diagonal matrix with diagonal elements equal to the inversed square root of the diagonal elements of D. In terms of orthogonormal states $\{|k>\}$, the matrix element of the static quark potential between states $|k>$ and $|k'>$ is

$$V_{kk'} = (D^{-\frac{1}{2}} S^+)_{ki} V_{ij} (S D^{-\frac{1}{2}})_{jk'} \tag{4-20}$$

By diagonalizing the matrix V, the eigenvalues are obtained and the lowest eigenvalue gives an upper boundary on the ground state energy of the heavy $\bar{q}q$ state.

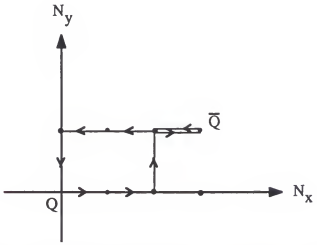

Figure 20. An example of $tr(Fi^{+}Fj)$ for $n_x = 2$, $n_y = 1$, and $Cij = 1$.

The quantities that must be calculated to obtain the matrix elements of M and V are $< tr(Fi^{+}Fj) >$ for all i and j. An example of $tr(Fi^{+}Fj)$ for $n_x = 2$, $n_y = 1$ is shown in Figure 20. Since the quark is placed at the origin and the antiquark is always in the x-y plane, $tr(Fi^{+}Fj)$ is the trace of a planar extended plaquette for any i and j. Because of the simplicity of the variational vacuum in eq. (4-2), it is always possible to use the Gross-Witten trick [21] to convert the expectation value of the trace of an extended plaquette to the expectation value

of the product of the traces of plaquettes contained in the extended plaquette. To explain the Gross-Witten trick, consider the expectation value of $\phi(\tilde{P})$ where

$\phi(\tilde{P})$ = tr (the extended plaquette shown in Figure 16(a))

$$= \mathrm{tr}(U_{p_1} U_{p_2}) \tag{4-21}$$

Since the variational vacuum, eq. (4-2), is a function of $\mathrm{tr}U_p$ only, it is invariant under the transformation

$$U_p \rightarrow V U_p V^{+} \tag{4-22}$$

where V is an element of SU(2) gauge group. The expectation value of $\phi(\tilde{P})$ then is

$$< \phi(\tilde{P}) > = \frac{\int [\prod_k dU_k] [\mathrm{tr}(U_{p_1} U_{p_2})] \exp(2\lambda \sum_p \mathrm{tr}U_p)}{\int [\prod_k dU_k] \exp(2\lambda \sum_p \mathrm{tr}U_p)}$$

$$= \frac{\int [\prod_k dU_k] [dV] [\mathrm{tr}(V U_{p_1} V^{+} U_{p_2})] \exp\{ 2\lambda \sum_p \mathrm{tr}U_p \}}{\int [\prod_k dU_k] \exp\{ 2\lambda \sum_p \mathrm{tr}U_p \}} \tag{4-23}$$

For SU(N) group

$$\int dV\, V_{il}\, V^{+}_{jk} = \frac{1}{N}\delta_{ik}\,\delta_{lj} \tag{4-24}$$

It then follows from eqs. (4-23) and (4-24) that

$$\langle \phi(\tilde{p}) \rangle = \frac{1}{2} \langle \mathrm{tr} U_{p_1} \bullet \mathrm{tr} U_{p_2} \rangle \tag{4-25}$$

The process of eq. (4-23) can be repeated to obtain the following general result: For an extended plaquette $f(\tilde{p})$ containing m plaquettes, $U_{p_1}, U_{p_2}, \cdots, U_{p_m}$, by applying the Gross-Witten trick(21) repeatedly it can be shown that

$$\langle \mathrm{tr}\, f(\tilde{p}) \rangle = \frac{1}{2^{m-1}} \langle \prod_{i=1}^{m} \mathrm{tr} U_{p_i} \rangle \tag{4-26}$$

Therefore, in the lattice calculation of static quark potential, the quantities that must be calculated are the expectation values of various products of the traces of plaquettes. In summary, the variational parameter λ is determined by minimizing the ground state energy, eq.(4-4a), then the potential, eq.(4-16), is evaluated by using the Gross-Witten trick(21) and the technique developed in Chapter 3.2. The results of static quark potentials for (n_x=1,n_y=3), (n_x=2,n_y=2), (n_x=2,n_y=3), and (n_x=3,n_y=3) as functions of coupling constant are shown in Figure 21.From the results of Figure 21, one

can locate the roughening transition point and extract the string tension for SU(2) Hamiltonian lattice gauge theory:

(a) The roughening transition point: In Section 2.1 of this chapter, it was pointed out that in lattice gauge theories a mass gap exists for the fluctuating flux tube and that mass gap easily can be overcome when the coupling strength decreases. Once the mass gap can be overcome, the flux tube starts to fluctuate and the rotational symmetry effectively is restored. In Figure 22, the equipotential surfaces of the static quark potentials, shown in figure 21, are drawn for various ξ values. The rotational symmetry is restored at $\xi_c = 0.26$,

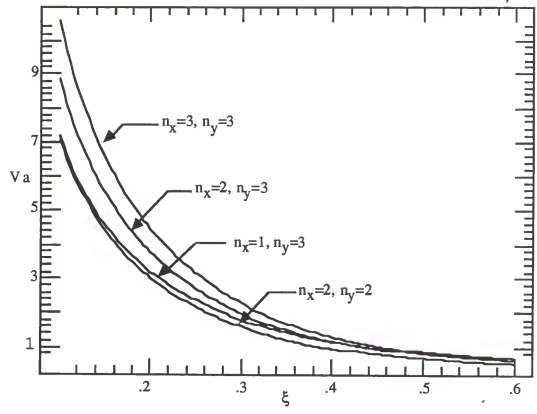

Figure 21. The results of static potentials for (n_x=1,n_y=3), (n_x=2,n_y=2), (n_x=2,n_y=3), and (n_x=3,n_y=3).

which is the critical coupling strength for the roughening transition. It remains rotationally symmetrical from $\xi = 0.26$ up to $\xi = 0.32$ After that, the perfect spheres start to be distorted slowly. Two statements should be made about the critical coupling strength $\xi_c = 0.26$:

(i) The result of the calculation applied here is very close to the value obtained by Monte Carlo calculation in Lagrangian formalism where $\xi_c \cong 0.22$, but quite different from the strong-coupling expansion result (41) in the Hamiltonian formalism where $\xi_c = 0.5$. As discussed in Chapter 2.2.2, for the same physical phenomena $g_H < g_L$. However the ratio of Λ_H and Λ_L is very close to 1, ξ_c^H in the Hamiltonian formalism is expected to be slightly higher than ξ_c^L in the Lagrangian formalism. On the other hand, for the Hamiltonian calculation the vacuum in the strong-coupling expansion is assumed to be rigid, and the variational vacuum allows magnetic fluctuation. Therefore, ξ_c calculated by strong-coupling expansion is expected to be higher than the result of the variational calculation.

(ii) Recent Monte Carlo calculations(31) of the glueball mass in the Hamiltonian formalism show that the strong-coupling expansion cannot give the correct result when $\xi \gtrsim \xi_0 \approx 0.3$ for SU(3). The ξ_0 should be slightly smaller than 0.3 for SU(2), because the correlation effect of SU(2) is stronger than that of SU(3). Since the glueball mass is inversely proportional to the fluctuated width of the flux tube and the reason for the strong-coupling expansion breaking down at the rough transition point in the calculation of string tension

was already explained in Chapter 3.1, we therefore conclude $\xi_c \approx \xi_o$, which is consistent with the result we obtained.

(b) The string tension: To find the string tension, the static quark potential is fitted to a simple form

$$V(L)\,a = (\sigma a^2)\frac{L}{a} + \delta + \frac{\alpha}{(L/a)} \qquad (4\text{-}27)$$

where a is the lattice spacing, σ is the string tension, the constant δ is due to the appearance of mass gaps in the lattice version of the string, and the Coulomb potential is due to a one-dimensional Casimir effect. Using the least-squares fitting, the string tension is extracted from the static quark potentials between a quark located at the origin and an antiquark at ($n_x = 1$, $n_y = 3$), ($n_x = 2$, $n_y = 2$), ($n_x = 2$, $n_y = 3$), ($n_x = 3$, $n_y = 3$), respectively, with the results shown in Figure 23. The data points of the string tension are shown only up to $\xi = 0.32$ because the variational vacuum is not accurate after that point. The scaling behavior exhibited by the string tension agrees very well with the expected asymptotic scaling line which yields

$$\Lambda_H = 0.009\sqrt{\sigma} \qquad (4\text{-}28)$$

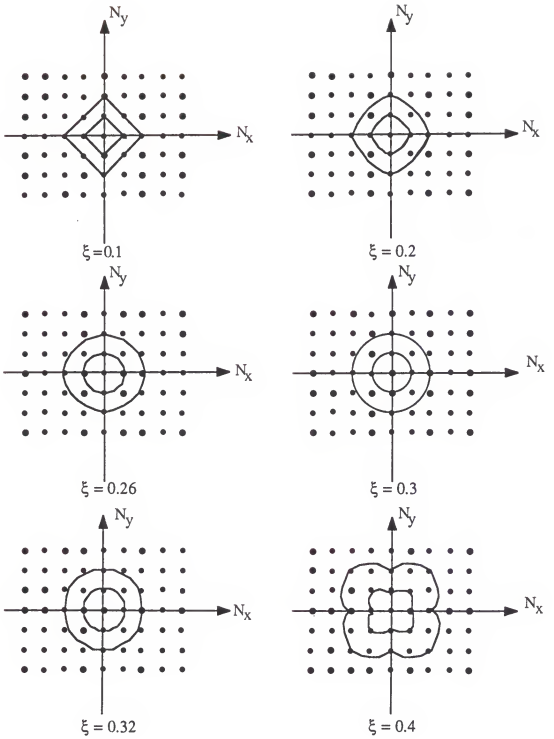

Figure 22. The equipotential surfaces for various values of ξ. The small dots denote lattice sites.

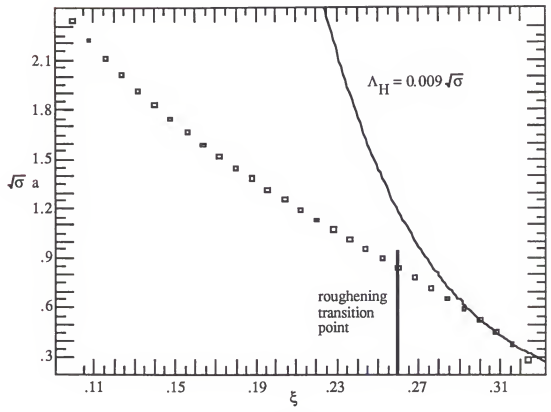

Figure 23. The string tension as a function of the coupling constant. The solid line is the expected asymptotic scaling line.

If

$$\Lambda_L = (0.0119 \pm 0.0015)\sqrt{\sigma} \tag{4-29}$$

which is the best estimation from the Lagrangian calculation.is adopted,[42] the ratio yielded is

$$\frac{\Lambda_H}{\Lambda_L} = 0.76 \pm 0.11 \qquad (4\text{-}30)$$

which is quite close to the theoretical prediction

$$\frac{\Lambda_H}{\Lambda_L} = 0.84 \qquad (4\text{-}31)$$

obtained by Hasenfratz and Hasenfratz.[33]

CHAPTER V
GLUEBALL MASS FOR SU(2) HAMIILTONIAN LATTICE GAUGE THEORY

A color singlet bound state of color gauge bosons is called a glueball state. In terms of string physics which were discussed in Chapter 4.2.1, glueball mass is inversely proportional to the fluctuating width of the flux tube, Thus, the glueball state is an excited collective mode of the system. Glueball masses with different J^{PC} assignments represents the energy differences between these J^{PC} low-lying excited states and the ground state. This chapter is devoted to calculations and discussions of 0^{++} glueball mass for SU(2) Hamiltonian lattice gauge theory.

To calculate the glueball mass, the variational vacuum--obtained in Chapter 4.1--is used as the ground state, and the trial lowest excited state is constructed to include correlations of up to two adjacent plaquettes. Calculations and results are presented in Section 5.1. Section 5.2 is reserved for discussion and comments regarding the results obtained in Section 1.

5.1. Calculations and Results

In Section 4.1, the trial ground state

$$\Psi_o = \exp\{ \lambda \sum_p \mathrm{tr} U_p \} \qquad (5\text{-}1a)$$

was proposed and the variational parameter λ was determined by minimizing the ground state energy per plaquette. If $|\Psi_1>$ is a trial first excited state of the form

$$|\Psi_1> = \bar{F}\,|\Psi_o> \qquad (5\text{-}1b)$$

where $\bar{F} = F - <F>$, with F is a linear combination of plaquette variables, and where the expectation of F, <F>, is taken with respect to the ground state $|\Psi_o>$, such that $|\Psi_1>$ is orthogonal to $|\Psi_o>$,

$$<\Psi_1|\Psi_o> = 0.$$

The variational parameters in $\bar{F}$ are determined by minimizing the lowest excited state energy as in

$$aE_1[\Psi_1] = \frac{<\Psi_1|aH|\Psi_1>}{<\Psi_1|\Psi_1>}$$

$$= \{ \frac{3\lambda}{8\xi} < \sum_p trU_p > + 4\xi\,(2 - trU_p) \}$$

$$+ (\frac{3\lambda}{8\xi} - 4\xi)\,\frac{1}{2}\frac{\partial}{\partial\lambda} \ln <\bar{F}^+\bar{F}>$$

$$+ \frac{1}{16\xi}\sum_k \sum_a \{ \frac{<[E^a_k, [E^a_k, F^+]]\,\bar{F}>}{<\bar{F}^+\bar{F}>} + \frac{<\bar{F}^+[E^a_k, [E^a_k, F]]>}{<\bar{F}^+\bar{F}>}$$

$$- 2 \frac{\langle [E_k^a, F^+] [E_k^a, F] \rangle}{\langle \tilde{F}^+ \tilde{F} \rangle} \} \qquad (5\text{-}2)$$

The derivation of eq. (5-2) is shown in Appendix B. The term in the first brace bracket is just the variational ground state energy. Since the glueball mass , M_g, is defined as the energy difference between the lowest excited state and the ground state, eq. (5-2) gives the glueball mass as

$$M_g a = a (E_1 - E_o)$$

$$= (\frac{3\lambda}{8\xi} - 4\xi) \frac{1}{2} \frac{\partial}{\partial \lambda} \ln \langle \tilde{F}^+ \tilde{F} \rangle$$

$$+ \frac{1}{16\xi} \sum_k \sum_a \{ \frac{\langle [E_k^a, [E_k^a, F^+]] \tilde{F} \rangle}{\langle \tilde{F}^+ \tilde{F} \rangle} + \frac{\langle \tilde{F}^+ [E_k^a, [E_k^a, F]] \rangle}{\langle \tilde{F}^+ \tilde{F} \rangle}$$

$$- 2 \frac{\langle [E_k^a, F^+] [E_k^a, F] \rangle}{\langle \tilde{F}^+ \tilde{F} \rangle} \} \qquad (5\text{-}3)$$

Eq. (5-3) can be simplified greatly by assuming the trial ground state, eq. (5-1a), is exact, then the glueball mass is[31,43]

$$M_g a = \frac{1}{2} \frac{\langle [F^+, [aH, F]] \rangle}{\langle \tilde{F}^+ \tilde{F} \rangle}$$

$$= -\frac{1}{4\xi}\sum_k\sum_a \frac{\langle (E_k^a F^+)(E_k^a F)\rangle}{\langle \bar{F}^+ \bar{F}\rangle} \qquad (5\text{-}4)$$

Here the second equality is obtained by using the integration by parts. The results of eqs. (5-3) and (5-4) should agree with each other in the strong-coupling region because the variational vacuum becomes the exact ground state in that region. However, different results should be expected in the intermediate coupling region. While eq. (5-4) is accepted commonly by most theorists[37,40,43] as the starting point for calculation of glueball mass, in this dissertation both expressions, eqs. (5-3) and (5-4), will be used simultaneously to perform the calculations of glueball mass. It is hoped that by comparing the two results some information about the physical system will be obtained.

To choose a projector F, notice that $\frac{1}{M_g a}$ is the correlation length in the unit of lattice spacing. As determined by the recent Monte Carlo calculations of glueball mass[37] for SU(N) lattice gauge theories with N=3, 4, 5, and 6, the estimated values of $\frac{1}{M_g a}$ in the intermediate coupling region are expected to be less than 1 for SU(2) lattice gauge theory. The projector, F, therefore, is chosen to include up to two adjacent plaquette correlations

$$F = \frac{1}{\sqrt{N_p}}\left\{\beta_1 \sum_p \phi_1(P) + \beta_2 \sum_{p_2} \phi_2(P_2) + \beta_3 \sum_{p_3} \phi_3(P_3)\right\} \qquad (5\text{-}5)$$

where β_i are variational parameters, $\phi_1(p)$ is the trace of a plaquette, $\phi_2(P_2)$ is the trace of an extended plaquette containing two adjacent plaquettes lying in the same plane, and $\phi_3(P_3)$ is the trace of an extended plaquette containing two adjacent plaquettes lying in two different planes. These three operators are shown in Figure 24.

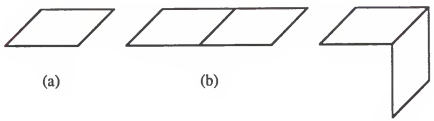

Figure 24. The operators used in the projector F
a) An elementary plaquette; b) Two adjacent plaquettes lying in the same plane; c) Two adjacent plaquettes lying in two different planes.

By using the projector of eq. (5-5), eq. (5-3) becomes

$$M_g a\,\xi = \frac{1}{\sum_{i,j=1}^{3} \beta_i^* D_{i,j} \beta_j} \{ \frac{1}{8} \sum_{i,j=1}^{3} \beta_i^* N_{i,j} \beta_j + \frac{1}{16} \sum_{i,j=1}^{3} \beta_i^* Q_{i,j} N_{i,j} \beta_j$$

$$+ (\frac{3\lambda}{8} - 4\xi^2) \sum_{i,j=1}^{3} \beta_i^* [-\frac{1}{2} \frac{\partial}{\partial\lambda} D_{ij}] \beta_j \} \qquad (5\text{-}6)$$

and eq. (5-4) becomes

$$M_g a\xi = \frac{1}{4} \frac{\sum_{i,j=1}^{3} \beta_i^* N_{ij} \beta_j}{\sum_{i,j=1}^{3} = \beta_i^* D_{ij} \beta_j} \tag{5-7}$$

where

$$N_{i,j} = -(1 + \delta_{i,2} + 3\,\delta_{i,3}) < \sum_k \sum_a (E_k^a \phi_i^*(0))(E_k^a \sum_p \phi(p)) > \tag{5-8}$$

$$D_{i,j} = (1 + \delta_{i,2} + 3\,\delta_{i,3}) \{ <\phi_i^*(0) \sum_p \phi_j(p)> - <\phi_i^*(0)> <\sum_p \phi_j(p)> \} \tag{5-9}$$

and

$$Q_{i,j} = \begin{bmatrix} 6 & \frac{15}{2} & \frac{15}{2} \\ \frac{15}{2} & 9 & 9 \\ \frac{15}{2} & 9 & 9 \end{bmatrix} \tag{5-10}$$

$\phi_i(o)$ denotes the trace of a i^{th} type of plaquette at a fixed position and the overall factor $(1 + \delta_{i,2} + 3\delta_{i,3})$ in N_{ij} and D_{ij} results from counting the number of the extended plaquettes on a lattice in the unit of the total number of plaquettes N_p. The minimization condition, $\frac{\partial}{\partial \beta_i} (M_g a\xi) = 0$, yields

$$\det \left| \frac{1}{8} N + \frac{1}{16} QD + \left(\frac{3\lambda}{8} - 4\xi^2\right) \frac{1}{2} \frac{\partial}{\partial \lambda} D - (M_g a\xi) D \right| = 0 \tag{5-11}$$

for eq. (5-6) and[43]

$$\det \left| \frac{1}{4} N - (\xi M_g a) D \right| = 0 \tag{5-12}$$

for eq. (5-7) for the nontrivial βi. The solutions of eq. (5-11) and eq. (5-12) will give the glueball mass for the cases of eqs. (5-3) and (5-4), respectively.

Since the color electric field operator, E^a_k, acts only on the common links of $\phi^*_i(o)$ and $\phi_j(p)$ in eq. (5-8), contributions to the matrix elements of N then come from adjacent and overlapped diagrams formed by any two plaquettes of various types in eq.(5-5). Using the Gross-Witten trick,(21) it can be shown that the contribution from the adjacent diagrams vanishes. To see this, consider an adjacent diagram formed by two plaquettes, $\tilde{U}_{p_1}$ and $\tilde{U}_{p_2}$, of various types in eq. (5-5) with one common link. Then

$$< \sum_k \sum_a (E^a_k \, tr\tilde{U}_{p_1}) (E^a_k \, tr\tilde{U}_{p_2}) > = < \sum_a tr(\frac{\tau^a}{2} \tilde{U}_{p_1}) tr(\frac{\tau^a}{2} \tilde{U}_{p_2}) >$$

$$= \frac{1}{4} [\, 2 < tr(\tilde{U}_{p_1} \tilde{U}_{p_2}) > - < tr\tilde{U}_{p_1} tr\tilde{U}_{p_2} >] \tag{5-13}$$

where the second equality is followed by the identity

$$\sum_a (\frac{\tau^a}{2})_{ij} (\frac{\tau^a}{2})_{km} = \frac{1}{4} (2 \, \delta_{i,m} \delta_{j,k} - \delta_{i,j} \, \delta_{k,m}) \tag{5-14}$$

and the result of eq. (5-13) vanishes, through eq. (4-26) which is obtained by using the Gross-Witten trick.(21) Therefore, for the matrix elements of N, only the overlapped diagrams of the matrix elements N_{ij}, which are shown in Tables 5 through 8, must be considered.

The matrix elements of D defined in eq. (5-9) signify the correlation effects. Although the variational vacuum is a product of the single-plaquette wavefunction, correlations will be involved through the lattice Bianchi identities even for disconnected diagrams, such as two separated plaquettes without a common link. Thus the calculations become complicated. To manage the calculations of the matrix elements of D, the following approximations are used: In the zeroth order, the correlation between two extended plaquettes (i,j = 2 and 3) is approximated by the correlation of an extended and an elementary plaquette. That is, for D22 the approximation yields

$$D_{22} = 2 \{ < \phi_2(o) \sum_p \phi_2(p) > - < \phi_2(o) > < \sum_p \phi_2(p) > \}$$

$$\approx 4 < \phi_1(o) > \{ < \phi_2(o) \sum_p \phi_1(p) > - < \phi_2(o) > < \sum_p \phi_1(p) > \}$$

$$\approx 4 < \phi_1(0) > \{ \frac{1}{2} \frac{\partial}{\partial \lambda} < \phi_2(0) > \}$$

$$\equiv D_{22}^{(0)} \qquad (5\text{-}15a)$$

where the Gross-Witten trick was used to get the second equality and

Table 5. The overlapped diagrams contributed to N_{1i} for i = 1, 2 and 3.

Matrix Element	Type of Diagrams	Number of Diagrams
N_{11}	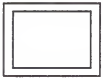	1
N_{12}	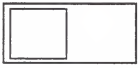	4
N_{13}		8

Table 6. The overlapped diagrams contributed to N_{22}.

Type of Diagrams	Number of Diagrams
	2
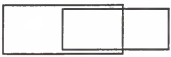	4
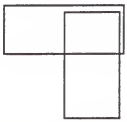	8

Table 7. The overlapped diagrams contributed to N_{23}.

Type of Diagrams	Number of Diagrams
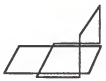	4
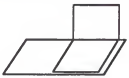	16
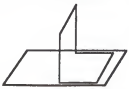	8

Table 8. The overlapped diagrams contributed to N_{33}.

Type of Diagrams	Number of Diagrams
	4
	8
	16
	8
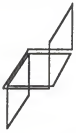	8
	16

the superscript on $D_{22}^{(0)}$ denotes the zeroth order approximation. In general, the zeroth order approximation gives

$$D_{ij}^{(0)} = \frac{1}{2}\left(1 + \delta_{i,2} + 3\,\delta_{i,3}\right)\left(1 + \delta_{j,2} + 3\,\delta_{j,3}\right)$$

$$< \phi_1(0) > \left(\frac{1}{2}\frac{\partial}{\partial\lambda} < \phi_i(0) > + \frac{1}{2}\frac{\partial}{\partial\lambda} < \phi_j(0) > \right)$$

$$\text{for } i \neq 1 \text{ and } j \neq 1 \qquad (5\text{-}15b)$$

To improve the zeroth order approximation, notice that the diagrams contributed to the correlations can be divided into three types: Disconnected (no common links), connected, and overlapped. The dominant contributions come from the overlapped diagrams. Therefore, to improve the approximation the contributions of the overlapped diagrams are calculated exactly and the difference between the results of the exact calculation and the zeroth order approximation for the overlapped diagrams is found. Finally, the difference is added to eq. (5-15b) to give

$$D_{ij} \approx D_{ij}^{(o)} + D_{ij}^{(1)} \qquad \text{for } i \neq 1 \text{ and } j \neq 1 \qquad (5\text{-}16)$$

Table 9. The matrix elements $D^{(1)}_{ij}$ for $i \neq 1$ and $j \neq 1$.

$D^{(1)}_{22} = \{\frac{1}{2}[<$  $>-<$  $>^2] +3[<$  $>-<$  $>^2]\} -[4<$  $>[<$  $>-<$  $><$  $>]\}$

$D^{(1)}_{32} = \{2[<$  $>-<$ $><$  $>] +4[<$  $>-<$  $><$  $>] +2[<$  $>-<$ $><$  $>]\} -\{8<$  $>[<$  $>-<$  $><$  $>]\}$

$D^{(1)}_{33} = \{[<$ $>-<$ $>^2] +2[<$ $>-<$ $>^2] +4[<$  $>-<$  $>^2] +2[<$ $>-<$ $>^2] +2[<$  $>-<$ $>^2] +4[<$  $>-<$  $>^2]\} -\{16<$ $>[<$ $>-<$ $><$ $>]\}$

where $D_{ij}^{(1)}$ are shown in Table 9. The matrix elements of D between elementary plaquettes and extended ones, i.e., Di1 for i = 1, 2 and 3, can be obtained exactly

$$D_{i1} = (1 + \delta_{i,2} + 3\delta_{i,3}) \{ \frac{1}{2} \frac{\partial}{\partial\lambda} < \phi_i(o) > \} . \qquad (5\text{-}17)$$

Now all the matrix elements of N and D are expressed in terms of the expectation values of some physical observables with respect to the trial ground state wavefunction, eq. (5-1a), and the method developed in Chapter 3.2 can be used to calculate these expectation values. Once the matrix elements of N and D are obtained, the glueball mass can be found by solving eqs. (5-11) and (5-12). The resultant glueball mass are shown in Figure 25. The squared dots represent the result of eq. (5-3), the triangular dots are those from eq. (5-4), and the solid lines are the expected asymptotic scaling lines. It can be seen from Figure 25 that both results exhibit an obvious tendency toward scaling, but the glueball mass in this calculation does not scale exactly along the expected asymptotic scaling line. By comparing the two curves in Figure 25, two remarks can be made:

(1) The two results coincide with each other for $\xi < 0.1$, which implies that the variational vacuum becomes the exact ground state for $\xi < 0.1$.

(2) In the intermediate region there is a significant difference between the two results. In particular, the curve falls down during the range of $0.22 \leq \xi \leq 0.30$ for the result of eq. (5-6) and $0.27 \leq \xi \leq 0.35$ for the result of

eq. (5-7). This implies that the trial ground state wavefunction, eq. (5-1a), is not good enough to assume it to be exact.

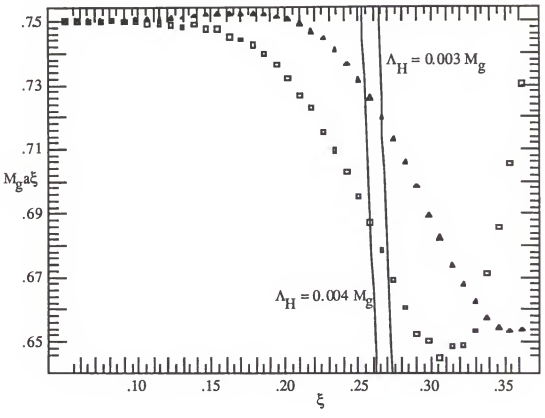

Figure 25. The result of glueball mass. The squared dots represent the result of eq. (5-3), the triangular dots that from eq. (5-4), and the solid lines are the expected asymptotic scaling lines.

5.2. Discussions and Comments

One intuitively derived suspicion to explain why the resultant glueball mass does not scale exactly along the expected asymptotic scaling line for a certain range of coupling constant is the following: The correlations contained in the

lowest excited trial state are not strong enough to yield the necessary collective mode. The extended plaquettes contained in the projector are all six-link plaquettes. Recent results obtained by Long, Robson, and Chin[44] for SU(3) glueball mass indicate that the six-link twisted plaquette (see Figure 26) may

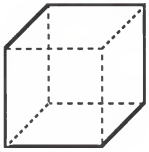

Figure 26. A six-link twisted plaquette.

play a more significant role than those included in this calculation.

Since glueball mass is a quantity determined through the collective mode, the scaling window is expected to be very small. However, it was pointed out by Chin and Karliner[45] that, in general, the ratio

$$R \equiv \frac{M_g}{\sqrt{\sigma}}$$

as a function of coupling constant should behave like the one depicted in Figure 27: The ratio R starts from the strong-coupling region (no scaling), exhibits a scaling window, and eventually diverges. Furthermore, the scaling window

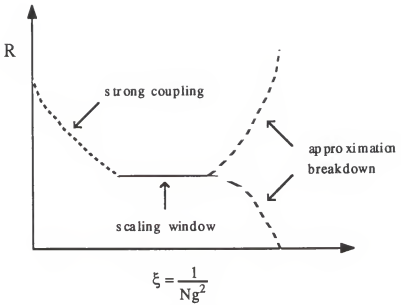

Figure 27. The behaviors of R in different coupling regions.
[This figure is taken from ref. (45).]

exhibited by the ratio R can cover a wider range of coupling constants than that exhibited by a single physical quantity M_g or $\sqrt{\sigma}$. [45] The ratio R therefore is computed and the result is shown in Figure 28. The scaling window is observed and the scaling behavior implies that

$$M_g = 2.86\sqrt{\sigma}$$

Previous estimates of the glueball mass in Lagrangian Monte Carlo calculations are $M_g = (3.5 \pm 1.2)\sqrt{\sigma}$ by Berg[46] and $M_g = (3.1 \pm 1.1)\sqrt{\sigma}$ by Bhanot and Rebbi.[42] The result obtain here agrees with those estimates.

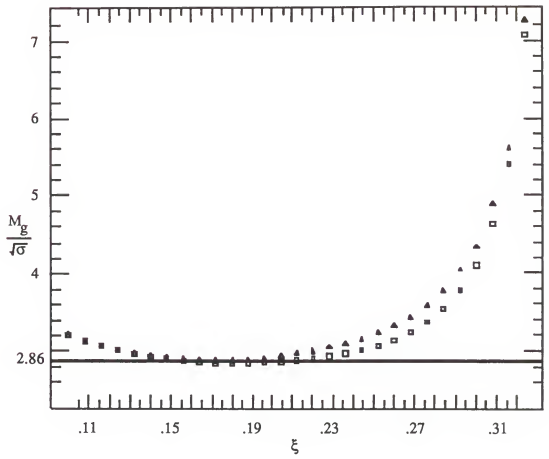

Figure 28. The ratio of glueball mass to the square root of string tension. The square dots are obtained by using the glueball mass of eq. (5-3), and the triangular dots are that from eq. (5-4).

CHAPTER 6
MONTE CARLO SIMULATION AND THE BIASED-SELECTION METHOD

Creutz[4] successfully applied Monte Carlo methods to the Lagrangian formalism of lattice gauge theories to demonstrate the coexistence of color confinement and asymptotic freedom in non-nonabelian gauge theories. Since then the Monte Carlo techniques have become an indispensable numerical tool for investigating the nonperturbative properties of lattice gauge theories. The Monte Carlo methods are an old technique, referred to as " importance sampling."[10] For example, consider an integral of the form

$$\langle O(U_p) \rangle = \frac{\int [\prod_k dU_k] \, O(U_p) \, \psi^2(U_p)}{\int [\prod_k dU_k] \, \psi^2(U_p)} \qquad (6\text{-}1)$$

in SU(2) Hamiltonian lattice gauge theory, where $\psi(U_p)$ is a known trial ground state wavefunction and $O(U_p)$ is a physical observable. If a 6^3 site lattice is used, there are 648 total linked. Since each link is associated with a group element of SU(2), there are 3 independent variables per link, with a total of 1944 variables. Equation (6-1) then becomes a 1944-dimensional integral. If a conventional numerical method, e.g. M-point quadrature formula, is used to do the integration, M^{1944} evaluations of the integrand are required. However

in the M^{1944} evaluations very few configurations contribute significantly to the expectation value $< O(U_p) >$ significantly, and much effort is wasted on the insignificant configurations. The difficulty in evaluating eq. (6-1) is shifted to the generation of important configurations. To state the problem precisely, the following probability density

$$P(U_p) = \frac{\psi^2(U_p)}{\int [\prod_k dU_k] \psi^2(U_p)} \tag{6-2}$$

is defined. Equation (6-1) then becomes

$$<O(U_p)> = \int [\prod_k dU_k] O(U_p) P(U_p) \tag{6-3}$$

Now the problem can be addressed: Without actually knowing what $P(U_p)$ is, how can an ensemble of configurations which are distributed according to $P(U_p)$ be generated? By viewing $P(U_p)$ as the stationary distribution of a Markov process, the above problem can be solved and the evaluation of eq. (6-1) be accomplished. There are two well-known, widely used computer algorithms--the Metropolis algorithm[10,47] and the heat bath algorithm[4,27] --which are adequate to process the Markov chain. These two algorithms are discussed in Section 6.1.

The tremendous consumption of computer time is always a problem in performing Monte Carlo calculations, even solely for the gluon sector. Thus,

improvement of the numerical technique is essential for a complete study of the theory. Section 6.2 focuses on this problem with yet another Monte Carlo technique, the Biased-Selection Monte Carlo method.(13)

6.1. The Markov Process

A common problem in lattice gauge theory is the evaluation of an integral of the form

$$\langle O(U_k) \rangle = \int [\prod_k dU_k] \, O(U_{k'}) \, P_s(U_{k''}) \tag{6-4a}$$

where $O(U_k)$ is a physical observable and $P_s(U_k)$ is analogous to the probability distribution function in statistical mechanics. In the Lagrangian formalism, eq. (6-4a) is a Euclidean expectation value of $O(U_k)$ with

$$P_s(U_k) = \frac{\exp [- S(U_p)]}{\int [\prod_k dU_k] \exp [- S(U_p)]} \tag{6-4b}$$

where $S(U_p)$ is the lattice action defined in eq. (2-5). In the Hamiltonian formalism, eq. (6-4a) is a variational estimate of a ground state expectation value of $O(U_k)$ with

$$P_s(U_k) = \frac{\psi^2 (U_k)}{\int [\prod_k dU_k] \, \psi^2 (U_k)} \tag{6-4c}$$

where $\psi(U_k)$ is a known trial ground state wavefunction. In the Metropolis and the heat bath algorithms, $P_s(U_k)$ is regarded as the stationary distribution of a Markov process. From knowing $\psi^2(U_k)$ or exp [- $S(U_k)$], a transition probability $W(U_k \rightarrow U_k')$ for changing the link value from U_k to U_k' is devised such that an arbitrary initial distribution $P_0(U_k)$ will evolve into $P_s(U_k)$ through the Markov process.

In both algorithms the starting point is an arbitrary configuration bearing with an initial distribution $P_0(U_k)$. A single-link variable then is altered and a new configuration $\{ U_k' \}$ is generated. The new configuration is accepted or rejected depending on whether the rules of the algorithm are satisfied or not. After all the link variables have been sampled, the entire lattice has been "swept through" once and a configuration $\{ C_i \}$ is established. Using the configuration established previously, this process is repeated N times to end up with N configurations. The expectation value $< O(U_k) >$ can then be estimated by

$$< O(U_k) > = \frac{1}{N} \sum_{i=1}^{N} O(\{C\}_i) \pm \sigma \qquad (6\text{-}5a)$$

where σ^2 is the variance

$$\sigma^2 = \frac{1}{N} \sum_{i=1}^{N} [O(\{C\}_i) - < O(U_k) >]^2 \qquad (6\text{-}5b)$$

However, there is an underlying assumption for eq. (6-5b): The N configurations are assumed to be mutually uncorrelated. To avoid the correlation between configurations in a Markov chain, the algorithm can be applied many times on $\{C\}_m$ until a new, statistically independent member of the stationary distribution, $\{C\}_{m+1}$, is generated. Since the standard deviation σ is inversely proportional to $\sqrt{N}$, the magnitude of N depends on how accurate is the result that is required. A typical value of N is about 3000.

6.1.1. The Metropolis Algorithm

For this algorithm, one starts with a configuration {C}, and a new configuration is generated through the following procedure:(47)

(a) The group element, U_k, associated with the link, k, in question is replaced by U_k' and all other links are held at their current values.

(b) The change in the action S (or in Ψ^2) is computed. If ΔS is less than zero (or $\Delta\Psi^2$ is larger than zero), the change is accepted. If ΔS is larger than zero (or $\Delta\Psi^2$ is less than zero), the change is accepted with the condition probability $\exp(-\Delta S)$ (or $\frac{\Psi^2(C')}{\Psi^2(C)}$). The transition probability $W(U_k \rightarrow U_k')$ here is assigned according to the detailed balance.

(c) The entire procedure then is repeated for the next link until the entire lattice is covered. This represents one Monte Carlo iteration.

(d) For the next Monte Carlo iteration, the previously established configuration is used as an initial configuration and then the steps (a) $\rightarrow$ (c) are repeated to establish another new configuration.

To show how the procedure eventually brings the system into the stationary probability distribution defined in eq. (6-4b) or (6-4c),[22,47] consider the relationship between the k^{th} and the $(k + 1)^{th}$ sweeps,

$$P_{k+1}(C) = \sum_{\{C'\}} P_k(C')\, W(C' \rightarrow C) + \Big(1 - \sum_{\{C'\}} W(C \rightarrow C')\Big)\, P_k(C)$$

$$= P_k(C) + \sum_{\{C'\}} \{\, P_k(C')\, W(C' \rightarrow C) - W(C \rightarrow C')\, P_k(C) \,\} \qquad (6\text{-}6a)$$

where $W(C \rightarrow C')$ is the probability for the transition $C \rightarrow C'$ with

$$\sum_{\{C'\}} W(C \rightarrow C') \leq 1 \qquad (6\text{-}6b)$$

For a stationary distribution,

$$P^S_{k+1}(C) = P^S_k(C) \qquad (6\text{-}7)$$

From eq. (6-6a), this implies the detailed balance

$$P^S_k(C')\, W(C' \rightarrow C) = P^S_k(C)\, W(C \rightarrow C') \qquad (6\text{-}8)$$

Now the transition probability in the Metropolis algorithm is

$$W(C \rightarrow C') = \begin{cases} 1 & \text{if } S(C') < S(C) \\ \exp\,[\, -(S(C') - S(C))\,] & \text{if } S(C') > S(C) \end{cases} \qquad (6\text{-}9a)$$

or

$$W(C \rightarrow C') = \begin{cases} 1 & \text{if } \psi^2(C') > \psi^2(C) \\ \dfrac{\psi^2(C')}{\psi^2(C)} & \text{if } \psi^2(C') < \psi^2(C) \end{cases} \qquad (6\text{-}9b)$$

So then

$$\frac{W(C \rightarrow C')}{W(C' \rightarrow C)} = \exp\left[- (S(C') - S(C)) \right] \qquad (6\text{-}10a)$$

or

$$\frac{W(C \rightarrow C')}{W(C' \rightarrow C)} = \frac{\psi^2(C')}{\psi^2(C)} \qquad (6\text{-}10b)$$

From eq. (6-8), this implies

$$P_k^S(C) = N \exp[- S(C)] \qquad (6\text{-}11a)$$

or

$$P_k^S(C) = N \psi^2(C) \qquad (6\text{-}11b)$$

where N is a constant which is determined by the normalization condition

$$\sum_{\{C\}} P_k^S(C) = 1 \qquad (6\text{-}11c)$$

Therefore, the algorithm provides the stationary probability distribution defined in eq. (6-4b) or (6-4c).

The Metropolis algorithm is very easy to implement because the explicit structure of the group measure can be ignored. However, in a weak coupling region, the correlation length of the system becomes large and most of the changes therefore would be routinely rejected. The configurations thus obtained are highly correlated. This is a practical problem in applying the Metropolis algorithm.

6.1.2. The Heat Bath Algorithm

Given the heat bath algorithm [4,30,48] and starting with a given configuration, a new configuration is generated through the following procedure:

(a) Starting from a link k, all of the links which interact with k have fixed U matrixes and provide a thermal background. There are six plaquettes interacting with k in the Lagrangian formalism, and four plaquettes in the Hamiltonian formalism.

(b) The group element, U_k, of link k is replaced with a new element, U_k', chosen randomly from the entire group with its probability proportional to the Boltzmann factor

$$dP(U') \sim \exp[\, -S(U') \,]\, dU' \qquad (6\text{-}12a)$$

in the Lagrangian formalism or to

$$dP(U') \sim \Psi^2 (U')\, dU' \qquad (6\text{-}12b)$$

in the Hamiltonian formalism S(U') (or Ψ^2 (U')) is evaluated with the link k having the value U'_k and all other interacting links fixed at their previous values.

(c) This procedure is applied to every link in the lattice to complete one iteration.

(d) For the next Monte Carlo iteration, the previously established configuration is taken as the initial configuration and then the steps (a) to (c) are followed to finish another Monte Carlo iteration.

The heat-bath algoritnm also satisfies the detailed balance. It is more effective than the Metropolis algorithm because for each iteration the system is brought closer to the stationary probability distribution. However, the heat bath is harder to implement because it needs the group measure explicitly in eq. (6-12a) or (6-12b). For complicated gauge groups like SU(3), it is tedious to work out eq. (6-12a) or (6-12b).[48] Thus, most Monte Carlo simulations in practice have turned to the Metropolis algorithm.

6.2. The Biased-Selection Monte Carlo Method

The Biased-Selection Monte Carlo method is a multi-dimensional extension of information sampling. It was introduced by Coldwell,[13] who used a simple form of this method to calculate the partition function of a hard disk system in statistical mechanics and more recently applied this method to calculate the potential between two helium atoms.[13]

In the Biased-Selection method, an integral such as

$$I(f) = \int dx_1\, dx_2 \cdots\, dx_n\ f(x_1, x_2, \cdots, x_n) \tag{6-13}$$

is estimated by

$$I(f) = \frac{1}{N} \sum_{i=1}^{N} \frac{f(\{x_1, x_2, \cdots, x_n\}_i)}{W_i} \pm \sigma_I \tag{6-14a}$$

where each configuration $\{x_1, x_2, \cdots, x_n\}_i$ is a set of values for $x_1, x_2, \cdots, x_n$ which was selected with probability W_i relative to the uniform and random distribution, and the standard deviation σ_I is given by the usual expression

$$\sigma_I^2 = \frac{1}{N} \sum_{i=1}^{N} \left(\frac{f(\{x\}_i)}{W_i} - I(f) \right)^2 \tag{6-14b}$$

Expectation values such as

$$< f > = \frac{\int dx_1\, dx_2 \cdots\, dx_n\, \psi^2(x_1, x_2, \cdots, x_n)\, f(x_1, x_2, \cdots, x_n)}{\int dx_1\, dx_2 \cdots\, dx_n\, \psi^2(x_1, x_2, \cdots, x_n)} \qquad (6\text{-}15)$$

are estimated by

$$< f > = \frac{\sum_{i=1}^{N} \psi^2(\{x_1, x_2, \cdots, x_n\}_i)\, f(\{x_1, x_2, \cdots, x_n\}_i) / W_i}{\sum_{i=1}^{N} \psi^2(\{x_1, x_2, \cdots, x_n\}_i) / W_i} \pm \sigma_f \qquad (6\text{-}16a)$$

with standard deviation

$$\sigma_f^2 = \frac{\sum_{i=1}^{N} [\psi^2(\{x\}_i)(f(\{x\}_i) - < f >) / W_i]^2}{[\sum_{i=1}^{N} \psi^2(\{x\}_i) / W_i]^2} \qquad (6\text{-}16b)$$

The standard deviation for $< f >$ is smaller than that for a ratio of two integrals since the same configurations are used for both the numerator and the denominator. W_i is determined by the guiding function used to choose the configurations. When the method for selecting configurations is a Markov chain, ψ^2 is used as the guiding function and eq. (6-16a) reduces to an average over equally weighted values of f. Therefore, the Markov chain is a subset of

the Biased-Selection method. But since correlations between configurations in the naive Markov chain are very high, eq. (6-16b) is not true.

The following section discusses in detail the application of this method to the particular case of calculating the ground state energy per plaquette for SU(2) Hamiltonian lattice gauge theory. The results demonstrate not only the accuracy, but also the speed, of the method.

6.2.1. Algorithms and Examples

As discussed in Section 4.1, if the wavefunction

$$\psi_0 = \exp\left(\lambda \sum_p \mathrm{tr} U_p\right) \tag{6-17}$$

is used as the trial ground state where λ is a variational parameter, then the ground state energy per plaquette is

$$a\,\mathcal{E}_0 = \left(\frac{3\lambda}{8\xi} - 4\xi\right) P(\lambda) + 8\xi \tag{6-18a}$$

where $\xi = \frac{1}{2g_o^2}$, and $P(\lambda)$ is the expectation value of plaquette

$$P(\lambda) = \frac{1}{N_p} \frac{\int \left[\prod_k dU_k\right] \left(\sum_p \mathrm{tr} U_p\right) \psi_0^2}{\int \left[\prod_k dU_k\right] \psi_0^2} \tag{6-18b}$$

The function $P(\lambda)$ in this form is the function to be evaluated using the Biased-Selection method.

There are two important ingredients in the following algorithm. The first is the guiding function ϕ for the biased selection of the configurations. It is not necessary for the guiding function to be the same as Ψ_0^2. In most cases, a single guiding function is used to cover certain ranges of λ in Ψ_0^2 if the physical properties implied by Ψ_0 do not change dramatically over those ranges of λ.

Another important nature of the algorithm lies in the partitions of lattice. When a function $f(x,y)$ is given approximately by $f_1(x)f_2(y)$, a product of probabilities (which corresponds to the case of using $f(x,y)$ to choose x and y) can be turned into a sum of probabilities by using $f_1(x)$ to choose x and $f_2(y)$ to choose y. In the case of the integration in eq. (6-18b) where the trial wavefunction, eq. (6-17), is a product of single-plaquette wavefunction, the integration can not be reduced to a single-plaquette integration. As discussed in Chapter 3.2, the correlations between various plaquettes will appear through the effect of Bianchi identities because the Haar measure is defined in the link space. However, the results of Chapter 3.2 showed that the effects of the Bianchi identities are very localized from the strong-coupling region down to the intermediate coupling region. The wavefunction, eq. (6-17), therefore can be sampled in terms of groups of plaquettes. The larger the effects of Bianchi identities, the bigger will be the number of plaquettes in a group. If a group of plaquettes can be sampled adequately, then a large step will have been taken toward sampling the full trial ground state wavefunction.

In the case discussed here, the number of plaquettes in a group is given as one. Starting with a particular plaquette, P, and a guiding function, ϕ, a configuration is generated by the following procedure:

(a) The group elements of SU(2) correspond to the unit vectors in four dimensions. The four links of the plaquette P are assigned values by randomly choosing values for the four-unit vectors associated with each link, L times.

(b) We then form

$$S(j) = \sum_{i=1}^{j} \phi_p [U_p(i)] \tag{6-19}$$

with $j \leq L$, and where $\phi = \prod_p \phi_p(U_p)$. Next a random number, R, is chosen between 0 and S(L) to pick up a set of link values, $U_n(k)$, $n \in p$, such that

$$\{ U_n(k) \mid U_p(k) = \prod_{n \in p} U_n(k),\ S(k-1) < R < S(k) \} . \tag{6-20a}$$

The probability for R being in the interval

$$S(k-1) < R < S(k) \tag{6-20b}$$

is exactly

$$P[U_p(k)] = \frac{\phi_p(U_p(k))}{\{ \frac{1}{L} S(L) \}} \tag{6-21}$$

Therefore, if $U_p(k)$ is chosen for plaquette P, the integrand must be divided by $P[\ U_p(k)\ ]$ to correct for this biasing.

(c) For the next plaquette, P', which has a common link, n, with plaquette P, we go through the same procedure (a) $\rightarrow$ (b) except that the common link n is held fixed in the previous value obtained from sampling the plaquette P.

(d) This procedure is repeated until the whole lattice is sampled, and a Monte Carlo iteration is established. For N_p plaquettes in the whole lattice, this process requires a total of LN_p plaquette evaluations and the probability of this configuration being selected is thus

$$W_i = \frac{\prod_{p_i=1}^{N_p} \phi_{p_i}}{\prod_{p_i=1}^{N_p} \{ \frac{1}{L} S_{p_i}(L) \}} \qquad (6\text{-}22)$$

The probability in eq. (6-22) indicates that the LNp choices with the partitions of lattice allow concentration on the region found only by L^{N_F} random choices without the partitions of lattice. Therefore, a product of probabilities has been converted into a sum.

(e) The process (a) $\rightarrow$ (d) can be repeated N times to accomplish N iterations. The N configurations thus established are statistically independent.

If $S_{p_i}(L)$ in eq. (6-22) was the same for each configuration, then eq. (6-16a) would reduce to a sum over equally weighted values of the integral just as in the

case of the Markov process. In addition, since each configuration (in the Biased-Selection method) is independent statistically, eq. (6-16b) is valid whenever there are enough configurations to estimate errors through such fluctuations. This leads to the definition of the effective number

$$N_{eff} = \frac{\{\sum_{i=1}^{N} \psi_0^2(i) / W_i\}^2}{\sum_{i=1}^{N} \psi_0^4(i) / W_i^2} \qquad (6\text{-}23)$$

which measures the number of configurations contributing non-zero amounts to eq. (6-16a). N_{eff} needs to be on the order of 30 or more for eq. (6-16b) to be valid. Some examples can now be discussed:

In 2 + 1 dimensions with free boundary condition, it was shown in Chapter 3.2 of this thesis, that because the Jacobian of transforming from the link space to plaquette space is the identity, the integration of eq. (6-18b) can be worked out analytically. The result is

$$P(\lambda) = -\frac{1}{\lambda} + 2\frac{I_0(4\lambda)}{I_1(4\lambda)} \qquad (6\text{-}24)$$

where $I_n(4\lambda)$ is the modified Bessel function of rank n defined in eq. (3-31b). To test the above algorithm, the Biased-Selection method is used to calculate $P(\lambda)$ defined in eq. (6-18b), and the results are compared with that of eq. (6-24). The guiding function ϕ used for the biased selection is

$$\phi(\beta) = \exp[\, 2\beta \sum_{p} \mathrm{tr} U_p \,] \qquad (6\text{-}25)$$

where $\beta = \frac{\lambda_1 + \lambda_2}{2}$ and β will be referred to as the weighting parameter. The considered range of the variational parameter $0 \le \lambda \le 0.6$ has been divided into three equal subintervals, and the midpoint of each of these subintervals has been chosen as the corresponding weighting parameter in the guiding function. The calculation was performed on a 6^2 lattice, L was set at 20, and the number of the established configurations was 1000. The result of this calculation is shown in Figure 29 (the squares) along with the analytical solution (the solid line). There are two striking features of this calculation: The first is that the Biased-Selection method produced the whole analytical result for the range of λ considered (the error is within the size of the squares in the figure). The second striking feature of this calculation is that the required CPU time was 20 minutes on a VAX 11-750. The need to divide the range of λ into subintervals arises from the fact that if the whole range of λ were used for the calculation with β = 0.3 (i.e., one guiding function), it would result in concentrating the sampling at higher values of the integrand near $\lambda = 0$ (due to the wider spreading of $\Psi_0^2(\lambda)$) and it would underestimate the integral near $\lambda = 0.6$ (due to the narrower spreading of $\Psi_0^2(\lambda)$).

In 3 + 1 dimensions, the calculation was performed on a 4^3 lattice by using the guiding function of eq. (6-25). In this calculation, the considered range of the variation parameter, $0 \le \lambda \le 0.6$, was divided into five equally spaced

intervals. L was set at 200 and the number of the established configurations was 3000. This calculation took 30 minutes of CPU time on an IBM 3090, and the result is shown in Figure 30. The error bars are too small to draw in the figure. The result obtained here is in best agreement with the Monte Carlo result obtained by Chin et al.(38)

6.2.2. Discussion and Comments

By comparing the two calculations presented above, one can see that the CPU time required in the case of 3 + 1 dimensions is considerably larger than that in 2 + 1 dimensions. The reason can be traced back to the extra degrees of freedom in 3 + 1 dimensions. As pointed out in Chapter 2.2, the correlation effect of a lattice system depends on the dimensionality of the lattice. Higher dimensions imply more correlations. It is expected, therefore, that the correlation effect will be more profound in 3 + 1 dimensions than that in 2 + 1 dimensions. The picture is more transparent if the calculations defined in the link space are transformed to that defined in the plaquette space. In the Hamiltonian formalism, the Jacobian for this transformation is the identity in 2 + 1 dimensions and the Bianchi identities in 3 + 1 dimensions. Therefore, the links in the whole lattice are correlated in 3 + 1 dimensions. However, when partitioning the lattice the number of plaquettes in a group was chosen to be one in the above calculations. This results in an inability to perform the biased-selection for 33% of the total number of plaquettes, those which are fixed during the procedure for the biased selection of the rest of the plaquettes.

To improve the above situation, the intuitively derived step would be to increase the number of plaquettes in a group which is the basic unit for the

partitions of the lattice. The calculation, while including three plaquettes in a group for the biased selection has been performed. The result indicates not only that the N_{eff} increases 40% more than in the previous case, but the interval of λ for the same weighting factor also increases.

The Biased-Selection method is more complex than the Markov chain. For quantum mechanical calculations, the ability to remove the Coulomb singularities (in atomic calculation) in $E(|x_1, x_2, \cdots, x_n|)$ with a guiding function other than ψ^2, along with the need for an accurate σ_E^2 in local energy calculation, provides a very good motive for tolerating the extra complexity.

Finally, two additional remarks can be made about the applications of the Biased-Selection method:

(a) The same configurations are used to find the expectation values for the different values of the variational parameter in the Biased-Selection method. Therefore, the errors in the difference between two expectation values are about on the same order of magnitude as the errors in the expectation values. The error in the derivative of a quantity is consequently reduced greatly compared with the case of the Markov chain.

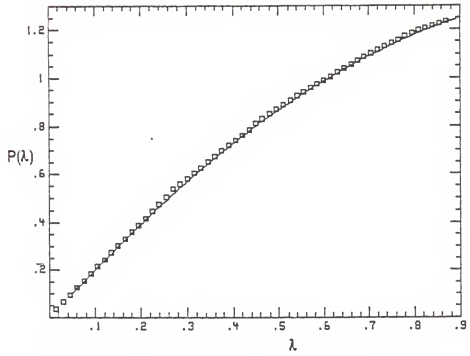

Figure 29. The expectation value of a plaquette in 2 + 1 dimensions. The solid line is the analytical result, and the squares are the Monte Carlo result.

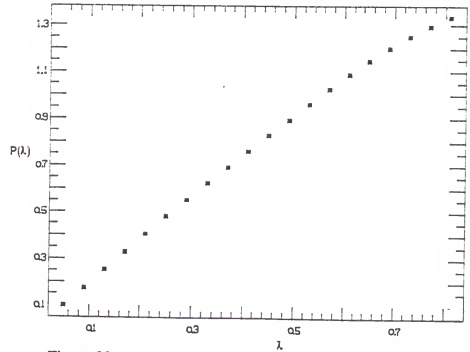

Figure 30. The plaquette expectation value in 3 + 1 dimensions.

(b) The Biased-Selection method is particularly suitable for the calculations of QCD at finite temperature and for a full study of the phase transitions that occur. Configurations can (without much difficulty) be generated on both sides of the phase transition, and included in the sums in eq. (6-16a). For a given set of parameters, an expectation value

$$\langle f \rangle = \frac{\sum_{i=1}^{n} \psi_i^2 f / W_{iu} + \sum_{i=1}^{n} \psi_i^2 f / W_{ic}}{\sum_{i=1}^{n} \psi_i^2 / W_{iu} + \sum_{i=1}^{n} \psi_i^2 / W_{ic}} \qquad (6\text{-}26)$$

where subscripts c and u refer to confined and unconfined phases respectively, automatically selects the important configurations from the appropriate region. Since in the Markov chain the W_i's are not calculated, these comparisons are much more difficult.

CHAPTER 7
CONCLUSION

Lattice group theories have offered a powerful approach for studies of quark confinement, hadronic spectroscopy, and ultrarelativistic heavy-ion collisions, which are closely related to the nonperturbative properties of the underlying continuum theory. In this dissertation an attemp has been made to study extensively the computation methods for lattice gauge theories and the physical properties of SU(2) Hamiltonian lattice gauge theory.

In Chapter 2, the formulation of SU(N) lattice gauge theory for both the Lagrangian and the Hamiltonian formalisms is established. Some conceptual issues regarding the formulations of lattice gauge theories are discussed in detail. A way to extract the continuum physics from a lattice calculation also is set up. Chapter 3 is devoted to discussions of the analytical calculation methods. The difficulty caused by the non-physical singularities in the calculations of strong-coupling expansion is discussed. It was pointed out that the variational calculations can circumvent the difficulty. An analytical method then was developed to accomplish the variational calculations of the static quark potential and the glueball mass for SU(2) Hamiltonian lattice gauge theory. By examining the analytical method in detail, the nature and general rules for applications of the method were established. In Chapter 4, the analytical method was applied to the variational calculation of static quark potential. From the static quark potential, it was possible to locate the rough transition point and

extract the string tension which is consistent with the expected asymptotic scaling line. The glueball mass for SU(2) Hamiltonian lattice gauge theory was calculated in Chapter 5 and the glueball mass in continuum physics was obtained from the scaling window of the ratio of glueball mass to the square root of string tension. In chapter 6, a new computer algorithm--the Biased-Selection method--was developed to perform Monte Carlo simulations. The numerical simulations performed in this dissertation by using the Biased-Selection method demonstrated that the new algorithm is accurate and also is reasonable in its consumption of computer time.

There are two main contributions contained in this dissertation: First, the establishment of new computation methods and, second, the results obtained in the variational study of SU(2) Hamiltonian lattice gauge theory. From a methodological viewpoint, two new computation methods are established through detailed examinations and practical demonstrations. One is the analytical method which permits performance of the variational calculations analytically. The other is a new computer algorithm, the Biased-Selection method, which enables performance of the Monte Carlo simulations correctly and efficiently.

The results achieved in the variational study of SU(2) Hamiltonian lattice gauge theory are the following:

(a) The roughening transition point is located at $\xi_c = 0.26$.

(b) The scaling string tension is obtained, and thus the scale parameter Λ_H is determined

$$\Lambda_H = 0.009\sqrt{\sigma}$$

(c) The scaling window for the ratio of glueball mass to the square root of string tension is observed, and it yields

$$M_g = 2.86\sqrt{\sigma}$$

These results are helpful in understanding the underlying physics of SU(2) Hamiltonian lattice gauge theory and the physics pictures thus established can possibly extend to the case of SU(3).

At present, the study of lattice gauge theory via the Hamiltonian technique is still under development and various problems of evaluating physical observables largely remain open. In particular, the fermion problem is a very challenging one. Fermions are not included in any calculation performed in this dissertation. This is mainly due to some surprisingly difficult problems met in the formulation of lattice fermions that have resisted resolution. It is generally believed that some conceptual breakthrough is needed to obtain a consistent formulation of lattice fermions. As mentioned in Section 2.1.2 , troubles encountered in trying to consistently include fermions in the formulation can be traced back to the distorted space-time symmetry of the Poincaré group in the lattice formulation. To pin down the problem, the first step is to formulate fermions in the random lattice where the space-time structure is more closed to the reality than that of the hypercubic lattice. Additional research activity currently being pursued by the author is concentrated on this direction.

REFERENCES

1. H. D. Politzer, Phys. Rev. Lett. **30**, 1346(1973).
   D. Grass and F. Wilczek, Phys. Rev. Lett. **30**, 1343(1973); Phys. Rev.**D8**, 3633(1973).

2. K. G. Wilson, Phys. Rev. **D10**, 2445(1974).

3. R. Savit, Rev. Mod. Phys. **52**, 453(1980).

4. M. Creutz, Phys. Rev. Lett. **45**, 313(1980).
   M. Creutz and K. J. M. Moriarty, Phys. Rev. **D26**, 2166(1982).

5. J. Kogut and L. Susskind, Phys. Rev. **D11**, 395(1975)

6. J. Bardeen, L. N. Cooper and J. R. Schrieffer, Phys. Rev. **108**, 1175(1957).

7. A. Chodos, R. J. Jaffe, K. Johnson, C. B. Thorn and V. F. Weisskopf, Phys. Rev. **D9**, 3471(1974).

8. W. A. Bardeen, M. S. Chanowitz, S. D. Drell, M. Weinstein and T. M. Yan, Phys. Rev. **D11**, 1094(1975).

9. H. E. Stanley, **Introduction to Phase Transition and Critical Phenomena**, Chapter 9, Oxford University Press, London, 1971.

10. J. M. Hammersly and D. C. Handscomb, **Monte Carlo Methods**, Methuen and Co., London, 1964.

11. G. G. Batrouni, Nucl. Phys. **B208**, 467, 12(1982).

12. D. Robson, **Plaquette-Space Integration**, Talk given in "The Workshop on Hamiltonian Lattice Gauge Theory and Monte Carlo Methods," March 16, 1987, Tallahassee, FL (Unpublished).

13. R. L. Coldwell, IJQC:QCS **11**,215(1977); Phys. Rev. **A7**,270(1973).

14. W. Pauli and F. Villara, Rev. Mod. Phys. **48**, 55(1935).

15. G. 't Hoft and M. Veltman, Nucl. Phys. **B44**, 189(1972).

16. J. Glimm and A. Jaffe, **Quantum Physics**, Springer-Verlag, New York, 1987 (second edition).
K. Osterwalder and E. Seiler, Ann. Phys. (N.Y.) **110**, 440(1978).
M. Lüscher, Commun. Math. Phys. **54**, 283(1977).

17. H. R. Quinn and M. Weinstain, Phys. Rev. **D34**, 2240(1986)
G. T. Bodwin and E. V. Kovacs, Phys. Rev. **D37**, 1008(1988).

18. M Lüscher, Commun. Math. Phys. **85**, 39(1982).
A. Phillips and D. Stone, Commun. Math. Phys. **85**, 39(1982).

19. N. S. Manton, Phys. Lett. **96B**, 328(1980).

20. C. B.Lang, P. Salomonson and B. S. Skagerstam, Phys. Lett. **100B**, 29(1981).

21. D. J. Gross and E. Witten, Phys. Rev. **D21**, 446(1980).

22. J. B. Kogut, Rev. Mod. Phys. **51**, 659(1979).

23. M. Creutz, Phys. Rev. Lett. **46**, 1441(1981).
I. G. Halliday and A. Schwimmer, Phys. Lett. **101B**, 327(1981).
J.Greensite and B. Lautrup, Phys. Rev. Lett. **47**, 9(1981).

24. G. Bhanot and M. Creutz, Phys. Rev. **D24**, 3212(1981).
G. Bhanot, Phys. Lett. **108B**, 337(1982).
G. Bhanot and R. Dashen, Phys. Lett. **113B**, 299(1982).

25. M. Creuz, Phys. Rev. **D15**, 1128(1977).

26. K. Huang, **Quarks, Leptons and Gauge Fields**, World Scientific, Singapore, 1982.

27. V. N. Gribov, Nucl. Phys. **B139**, 1(1978).

28. R. Jackiw and C. Rebbi, Phys. Rev. Lett. **37**, 172(1976).
C. G. Callan, R. F. Dashen, and D. J. Gross, Phys. Lett. **63B**, 334(1976)

29. W. E. Caswell, Phys. Rev. Lett. **33**, 244(1974).
D. R. Jones, Nucl. Phys. **B75**, 531(1974).

30. M. Creutz, **Quarks, Gluons and Lattices**, Chapter 13, Cambridge University Press, London, 1983.

31. A. Hasenfratz and P. Hasenfratz, Phys. Lett. **93B**, 165(1980).

32. R. Balian, J. M. Drouffe, and C. Itzykson, Phys. Rev. **D11**,2104(1975).

33. G. Münster and P. Weisz, Nucl. Phys. **B180**[FS2], 13(1981)
A. Hasenfratz, E. Hasenfratz, and P. Hasenfratz, **B180**[FS2], 353(1981)

34. M. B. Halpern, Phys. Rev., **D19**, 517(1979).

35. J. B. Kogut, D. K. Sinclair, R. B. Pearson, J. L. Richardson, and J. Shigemitsu, Phys. Rev. **D23**, 2945(1981).
J. B. Kogut and D. K. Sinclair, Phys. Rev. **D24**, 1610(1981).

36. G. Arfken, **Mathematical Methods for Physicists**, Academic Press, New York, 1973.

37. S. A. Chin, C. Long, and D. Robson, Phys. Rev. Lett. **57**, 2779(1986).

38. S. A. Chin, O. S. Van Rosemalen, G. A. Umland and S. E. Koonin, Phys. Rev. **D31**, 3201(1985).

39. M. Lüscher, Nucl. Phys. **B180**[FS2], 317(1981).

40. S. P. Tonkin, Nucl. Phys. **B292**, 573(1987).

41. R. P. Feynman, Nucl. Phys. **B188**, 579(1981).
J. P. Greensite, Nucl. Phys. **B158**, 469(1979).

42. B. Berg, A. Billoire, and C. Rebbi, Ann. Phys. **142**, 185(1982).
G. Bhanot and C. Rebbi, Nucl. Phys. **B180**, 469(1981).

43. H. Arisu, M. Kato, and T. Fujiwaru, Prog. Theor. Phys. **70**, 229(1983).

44. C. Long, D. Robson, and S. A. Chin, Phys. Rev. **D37**, 3006(1988).

45. S. A. Chin and M. Karliner, Phys. Rev. Lett. **58**, 1803(1987).

46. B. Berg, Phys. Lett. **97B**, 401(1980).

47. N. Metropolis, A. W. Rosenbluth, M. N. Rosenbluth, A. H. Teller, and E. Teller, Phys. Rev. **21**,1087(1953).

48. E. Pietarinen, Nucl. Phys. **B190**[FS3], 349(1981).
N. Cabibbo and E. Marinari, Phys. Lett. **119B**, 387(1982).

APPENDIX A
THE DERIVATION OF EQ. (4-14)

If

$$| i > \equiv \Psi^{+}(n_x, n_y)\, F_i\, \Psi(0, 0)\, | \psi_0 >$$

and

$$<U_p | \psi_0 > = \exp\{ \frac{S}{2} \}$$

with $S \equiv 2\lambda \sum_p \mathrm{tr} U_p$, then the matrix element of between states $| i >$ and $| j >$ for the color-electric term in the Hamiltonian is

$$< i | \sum_k \sum_a E_k^a E_k^a | j >$$

$$= \int [\prod_k dU_k] \{ \exp(\frac{S}{2}) [E_k^a E_k^a] \exp(\frac{S}{2}) \}$$

$$= - \int [\prod_k dU_k] \{ (E_k^a \exp(\frac{S}{2})) (E_k^a \exp(\frac{S}{2})) F_j^{+} F_i$$

$$+ \exp(\frac{S}{2}) (E_k^a F_j^{+}) F_i (E_k^a \exp(\frac{S}{2}))$$

$$+ (E_k^a \exp(\frac{S}{2})) F_j^{+} (E_k^a F_i) \exp(\frac{S}{2})$$

$$+ \exp(\frac{S}{2}) (E^a_k F^+_j) (E^a_k F_i) \exp(\frac{S}{2}) \} \qquad \text{(A-1)}$$

where the second equality is obtained by using the integration by parts, and the summation in the indices, k and a, is implied. The first term in the bracket of eq.(A-1) can be rewritten as

$$- \int [\prod_k dU_k] \{ (E^a_k \exp(\frac{S}{2})) (E^a_k \exp(\frac{S}{2})) F^+_j F_i \}$$

$$= - \langle \psi_0 | (E^a_k \ln\psi_0)(E^a_k \ln\psi_0) F^+_j F_i | \psi_0 \rangle$$

$$= \frac{1}{2} \langle \psi_0 | (E^a_k E^a_k \ln\psi_0) F^+_j F_i | \psi_0 \rangle$$

$$+ \frac{1}{2} \int [\prod_k dU_k] \exp(\frac{S}{2}) (E^a_k F^+_j) F_i (E^a_k \exp(\frac{S}{2}))$$

$$+ \frac{1}{2} \int [\prod_k dU_k] \exp(\frac{S}{2}) F^+_j (E^a_k F_i) (E^a_k \exp(\frac{S}{2})) \qquad \text{(A-2)}$$

Substituting eq. (A-2) into eq. (A-1), it yields

$$\langle \psi_0 | F^+_j E^a_k E^a_k F_i | \psi_0 \rangle$$

$$= \frac{1}{4} \langle \psi_0 | \{ [E^a_k, [E^a_k, S]] \} F^+_j F_i | \psi_0 \rangle$$

$$-\frac{1}{2}\int [\prod_k dU_k] \exp(\frac{S}{2}) (E_k^a F_j^+) F_i (E_k^a \exp(\frac{S}{2}))$$

$$-\frac{1}{2}\int [\prod_k dU_k] \exp(\frac{S}{2}) F_j^+ (E_k^a F_i) (E_k^a \exp(\frac{S}{2}))$$

$$-\int [\prod_k dU_k] \exp(\frac{S}{2}) (E_k^a F_j^+) (E_k^a F_i) \exp(\frac{S}{2}) \qquad \text{(A-3)}$$

-Consider the following term in eq. (A-3)

$$\int [\prod_k dU_k] \exp(\frac{S}{2}) (E_k^a F_j^+) F_i (E_k^a \exp(\frac{S}{2}))$$

$$= -\int [\prod_k dU_k] (E_k^a \exp(\frac{S}{2})) (E_k^a F_j^+) F_i \exp(\frac{S}{2})$$

$$-\int [\prod_k dU_k] \exp(\frac{S}{2}) (E_k^a E_k^a F_j^+) F_i \exp(\frac{S}{2})$$

$$-\int [\prod_k dU_k] \exp(\frac{S}{2}) (E_k^a F_j^+) (E_k^a F_i) \exp(\frac{S}{2})$$

i. e., by using the integration by parts, one can show that

$$\int [\prod_k dU_k] \exp(\frac{S}{2}) (E_k^a F_j^+) F_i (E_k^a \exp(\frac{S}{2}))$$

$$= -\frac{1}{2}\int [\prod_k dU_k] \exp(\frac{S}{2}) (E_k^a E_k^a F_j^+) F_i \exp(\frac{S}{2})$$

$$-\frac{1}{2}\int [\prod_k dU_k] \exp(\frac{S}{2}) (E^a_k F^+_j) (E^a_k F_i) \exp(\frac{S}{2}) \qquad \text{(A-4)}$$

Using a similar procedure of obtaining eq. (A-4), it yields

$$\int [\prod_k dU_k] \exp(\frac{S}{2}) F^+_j (E^a_k F_i) (E^a_k \exp(\frac{S}{2}))$$

$$= -\frac{1}{2}\int [\prod_k dU_k] \exp(\frac{S}{2}) F^+_j (E^a_k E^a_k F_i) \exp(\frac{S}{2})$$

$$-\frac{1}{2}\int [\prod_k dU_k] \exp(\frac{S}{2}) (E^a_k F^+_j) (E^a_k F_i) \exp(\frac{S}{2}) \qquad \text{(A-5)}$$

Substituting eqs. (A-4) and (A-5) into eq. (A-3), the result is

$$\langle \psi_0 | F^+_j E^a_k E^a_k F_i | \psi_0 \rangle$$

$$= \frac{1}{4} \langle \psi_0 | \{ [E^a_k, [E^a_k, S]] \} F^+_j F_i | \psi_0 \rangle$$

$$+ \frac{1}{4} \langle \psi_0 | F^+_j [E^a_k, [E^a_k, F_i]] | \psi_0 \rangle$$

$$+ \frac{1}{4} \langle \psi_0 | [E^a_k, [E^a_k, F^+_j]] F_i | \psi_0 \rangle$$

$$- \frac{1}{2} \langle \psi_0 | [E^a_k, F^+_j] [E^a_k, F_i] | \psi_0 \rangle \qquad \text{(A-6)}$$

Equation. (4-14) can be obtained by working out each term in eq.(A-6) explicitly.

APPENDIX B
THE DERIVATION OF EQ. (5-2)

If

$$| \psi_1 > \equiv \tilde{F} | \psi_0 > = (F - <F>) | \psi_0 > \qquad \text{(B-1)}$$

where F is a function of plaquette variables, and the expectation value of F, <F>, is taken with respect to $| \psi_0 >$, then

$$a E_1 \equiv \frac{<\psi_1 | a H | \psi_1>}{<\psi_1 | \psi_1>} = \frac{<\psi_1 | a H | \psi_1> / <\psi_0 | \psi_0>}{<\psi_1 | \psi_1> / <\psi_0 | \psi_0>} \qquad \text{(B-2)}$$

and

$$\frac{<\psi_1 | \psi_1>}{<\psi_0 | \psi_0>} = <\tilde{F}^{+} \tilde{F}> \qquad \text{(B-3)}$$

with

$$aH = \frac{1}{4\xi} \sum_k \sum_a E_k^a E_k^a + 4\xi \sum_p (2 - \mathrm{tr} U_p) \qquad \text{(B-4)}$$

The contribution of color-electric term to eq. (B-2) is

$$\frac{1}{4\xi}\frac{\langle\psi_1 | \sum_k \sum_a E_k^a E_k^a | \psi_1\rangle}{\langle\psi_1 | \psi_1\rangle}$$

$$= \frac{3\lambda}{8\xi}\{ \langle \sum_p \mathrm{tr}U_p\rangle + \frac{1}{2}\frac{\partial}{\partial\lambda}\ln\langle\bar{F}^+\bar{F}\rangle \}$$

$$+ \frac{1}{16\xi}\frac{1}{\langle\bar{F}^+\bar{F}\rangle}\sum_k\sum_a \{ \langle [E_k^a, [E_k^a, F^+] \bar{F}\rangle + \langle\bar{F}^+ [E_k^a, [E_k^a, F]\rangle$$

$$- 2\langle [E_k^a, F^+] [E_k^a, F]\rangle \} \qquad \text{(B-5)}$$

by using eq. (A-6) in Appendix A directly. It is straightforward to calculate the contribution of color-magnetic term to eq. (B-2), and the result is

$$4\xi\frac{\langle\psi_1 | \sum_p (2 - \mathrm{tr}U_p) | \psi_1\rangle}{\langle\psi_1 | \psi_1\rangle}$$

$$= 4\xi (\langle \sum_p (2 - \mathrm{tr}U_p)\rangle - \frac{1}{2}\frac{\partial}{\partial\lambda}\ln\langle\bar{F}^+\bar{F}\rangle) \qquad \text{(B-6)}$$

Combining eqs. (B-5) and (B-6), the result of eq. (5-2) is then obtained.

BIOGRAPHICAL SKETCH

Ming Chang Huang, 34, was born in Taiwan, Republic of China. He was graduated from Chung-Yuan Christian University in Taiwan in 1978 with a bachelor's degree in physics and from Fu-Jen Catholic University in Taiwan in 1980, with a master's degree in theoretical solid state physics.

His major research interests are theoretical physics and analytical philosophy. Huang will return to Taiwan right after obtaining the Ph.D. degree, not only because he has a strong desire to serve his country, but also because there he can continue the research both in theoretical physics and analytical philosophy.

I certify that I have read this study and that in my opinion it conforms to acceptable standards of scholarly presentation and is fully adequate, in scope and quality, as a dissertation for the degree of Doctor of Philosophy.

F.E. Dunnam, Chair
Professor of Physics and
Astronomy

I certify that I have read this study and that in my opinion it conforms to acceptable standards of scholarly presentation and is fully adequate, in scope and quality, as a dissertation for the degree of Doctor of Philosophy.

R.L. Coldwell, Cochair
Associate Professor of Physics

I certify that I have read this study and that in my opinion it conforms to acceptable standards of scholarly presentation and is fully adequate, in scope and quality, as a dissertation for the degree of Doctor of Philosophy.

J. Dufty
Professor of Physics

I certify that I have read this study and that in my opinion it conforms to acceptable standards of scholarly presentation and is fully adequate, in scope and quality, as a dissertation for the degree of Doctor of Philosophy.

D. Robson
Professor of Physics
Florida State University

I certify that I have read this study and that in my opinion it conforms to acceptable standards of scholarly presentation and is fully adequate, in scope and quality, as a dissertation for the degree of Doctor of Philosophy.

M. Katoot
Assistant Research Scientist
in Space Astronomy Laboratory

I certify that I have read this study and that in my opinion it conforms to acceptable standards of scholarly presentation and is fully adequate, in scope and quality, as a dissertation for the degree of Doctor of Philosophy.

J. Keesling
Professor of Mathematics

This dissertation was submitted to the Graduate Faculty of the Department of Physics in the College of Liberal Arts and Sciences and to the Graduate School and was accepted as partial fullfillment of the requirements for the degree of Doctor of Philosophy.

August, 1988

Dean, Graduate School